Electronic Supplementary Material (ESI) for Physical Chemistry Chemical Physics.

Supporting Information for: Gaseous Inhibition of the Transsulfuration Pathway by Cystathionine β-Synthase

Neil R. McFarlane[a], Jiangli Gui[a], Julianna Oláh[b], Jeremy N. Harvey[a]

[a] Department of Chemistry
KU Leuven
B-3001 Leuven Celestijnenlaan 200f- box 2404, Belgium
E-Mail: neilrory.mcfarlane@kuleuven.be
E-Mail: jeremy.harvey@kuleuven.be
[b] Department of Inorganic and Analytical Chemistry
Budapest University of Technology and Economics
H-1111 Budapest, Műegyetem rakpart 3.
E-Mail: olah.julianna@vbk.bme.hu

Additional Methodology

Complete Basis Set Limit Extrapolation Scheme

To facilitate the extrapolation, two basis set combinations (TZVPP/TZVP/SVP & QZVPP/TZVP/SVP) were selected as shown in ***Table S1***, noting that the extrapolation scheme was only extended to heme iron.

Table S1: *The three basis set combinations used throughout the quantum chemical calculations. Basis set combination TZVP/SVP was used for all geometry optimisations, and basis set combinations TZVPP/TZVP/SVP and QZVPP/TZVP/SVP were used for basis set extrapolations on DLPNO-CCSD(T_1) calculations.*

Basis Set Combination	**Atom**					
	Fe	*N*	*O*	*S*	*C*	*H*
TZVP/SVP	Def2-TZVP	Def2-SVP	Def2-SVP	Def2-SVP	Def2-SVP	Def2-SVP
TZVPP/TZVP/SVP	ZORA-Def2-TZVPP	ZORA-Def2-TZVP	ZORA-Def2-TZVP	ZORA-Def2-TZVP	ZORA-Def2-TZVP	ZORA-Def2-SVP
QZVPP/TZVP/SVP	ZORA-Def2-QZVPP	ZORA-Def2-TZVP	ZORA-Def2-TZVP	ZORA-Def2-TZVP	ZORA-Def2-TZVP	ZORA-Def2-SVP

The CBS limit extrapolations for both the electronic and correlation energy were calculated using ***Equation (S1)*** and ***Equation*** **(S2)**, and the total CBS limit extrapolated DLPNO-CCSD(T_1) electronic energy was calculated with ***Equation (S3)***. Here, there are two constants, $a = 7.88$ and $b = 2.97$, and $X = 3$ and $Y = 4$ represent the cardinal numbers of the def2 basis set hierarchies.[1]

$$E_{elec.}^{CBS} = \frac{e^{a\cdot\sqrt{X}} \cdot E_{elec.}^{(X)} - e^{a\cdot\sqrt{Y}} \cdot E_{elec.}^{(Y)}}{e^{a\cdot\sqrt{X}} - e^{a\cdot\sqrt{Y}}} \qquad \textbf{(S1)}$$

$$E_{corr.}^{CBS} = \frac{X^b \cdot E_{corr.}^{(X)} - Y^b \cdot E_{corr.}^{(Y)}}{X^b - Y^b} \qquad \textbf{(S2)}$$

$$E_{DLPNO-CCSD(T1)}^{CBS} = E_{elec.}^{CBS} + E_{corr.}^{CBS} \qquad \textbf{(S3)}$$

Additional Figures and Tables

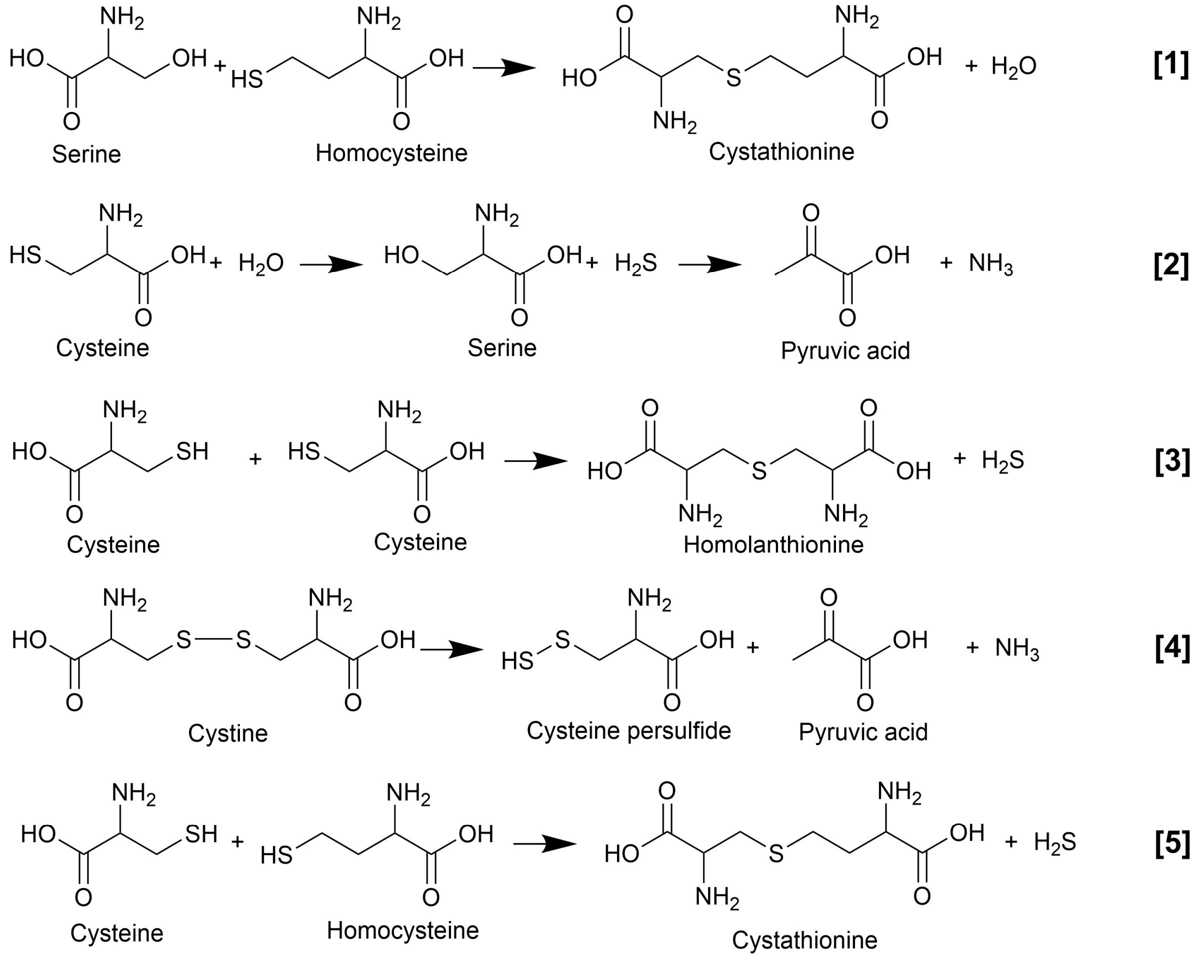

Figure S1: *The set of reactions observed in human CBS. Reaction* ***[1]*** *is the canonical reaction found in human CBS, and reactions* ***[2]****-****[5]*** *are the side reactions found in human CBS. All species are given in their neutral form.*

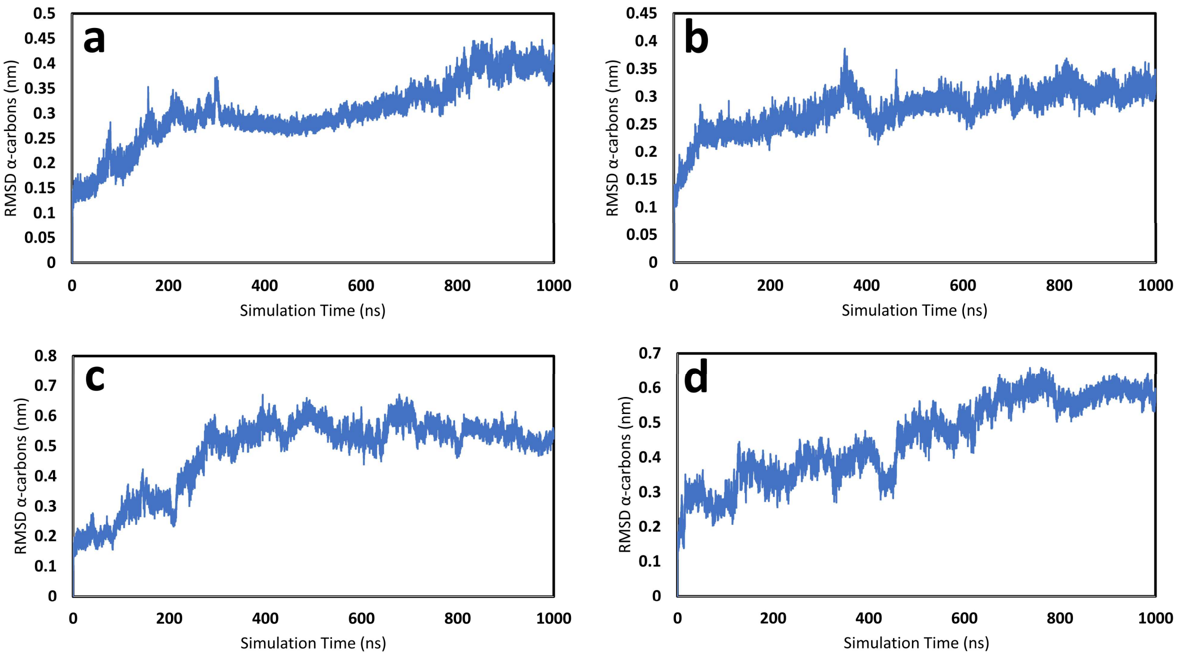

***Figure S2**: **a.** RMSD of the α-carbons averaged across both chains A and B for the first 1000 ns simulation of **A**; **b.** RMSD of the α-carbons averaged across both chains A and B for the second 1000 ns simulation of **A**; **c.** RMSD of the α-carbons averaged across both chains A and B for the first 1000 ns simulation of **C**; **d.** RMSD of the α-carbons averaged across both chains A and B for the second 1000 ns simulation of **C**.*

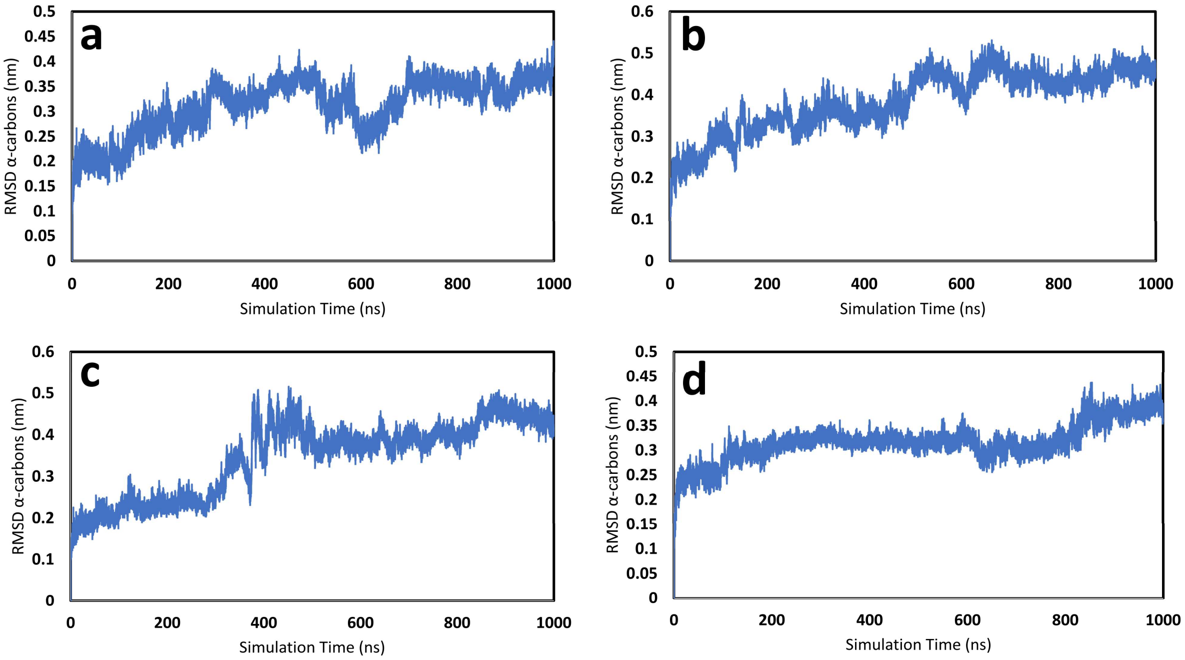

***Figure S3: a.** RMSD of the α-carbons averaged across both chains A and B for the first 1000 ns simulation of **E**; **b.** RMSD of the α-carbons averaged across both chains A and B for the second 1000 ns simulation of **E**; **c.** RMSD of the α-carbons averaged across both chains A and B for the first 1000 ns simulation of **F**; **d.** RMSD of the α-carbons averaged across both chains A and B for the second 1000 ns simulation of **F**.*

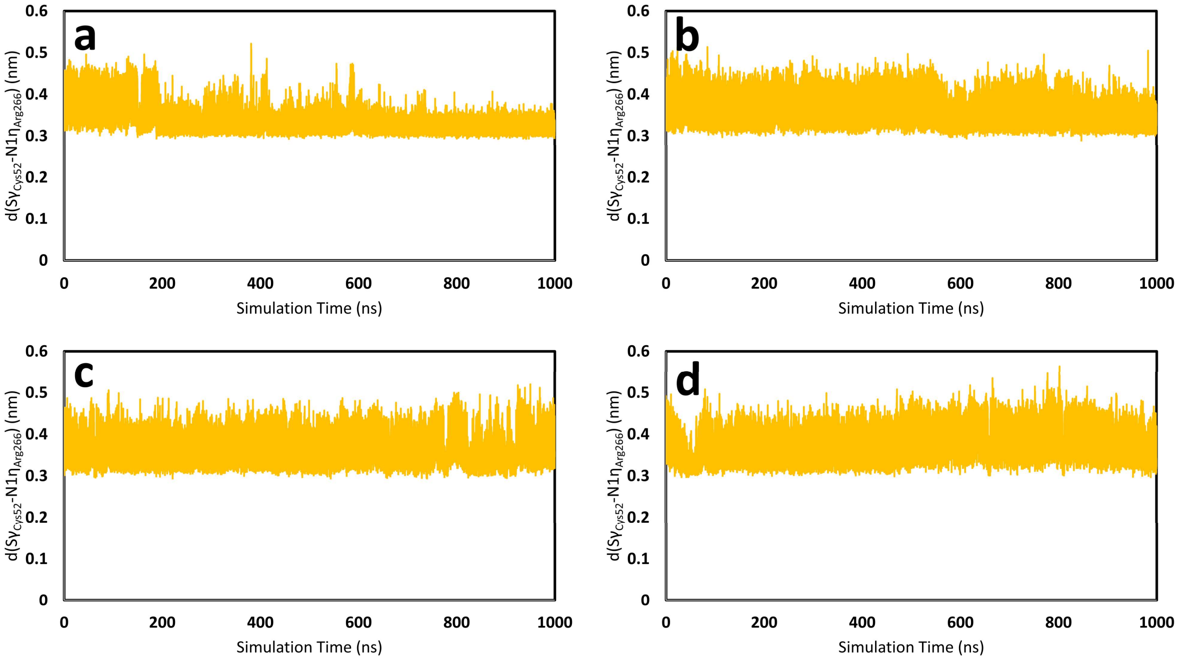

Figure S4: ***a.*** *variation of d(S*γ_{Cys52}*-N1*η_{Arg266}*) for chain A for the first 1000 ns simulation of* ***A****;* ***b.*** *variation of d(S*γ_{Cys52}*-N1*η_{Arg266}*) for chain B for the first 1000 ns simulation of* ***A****;* ***c.*** *variation of d(S*γ_{Cys52}*-N1*η_{Arg266}*) for chain A for the second 1000 ns simulation of* ***A****;* ***d.*** *variation of d(S*γ_{Cys52}*-N1*η_{Arg266}*) for chain B for the second 1000 ns simulation of* ***A****.*

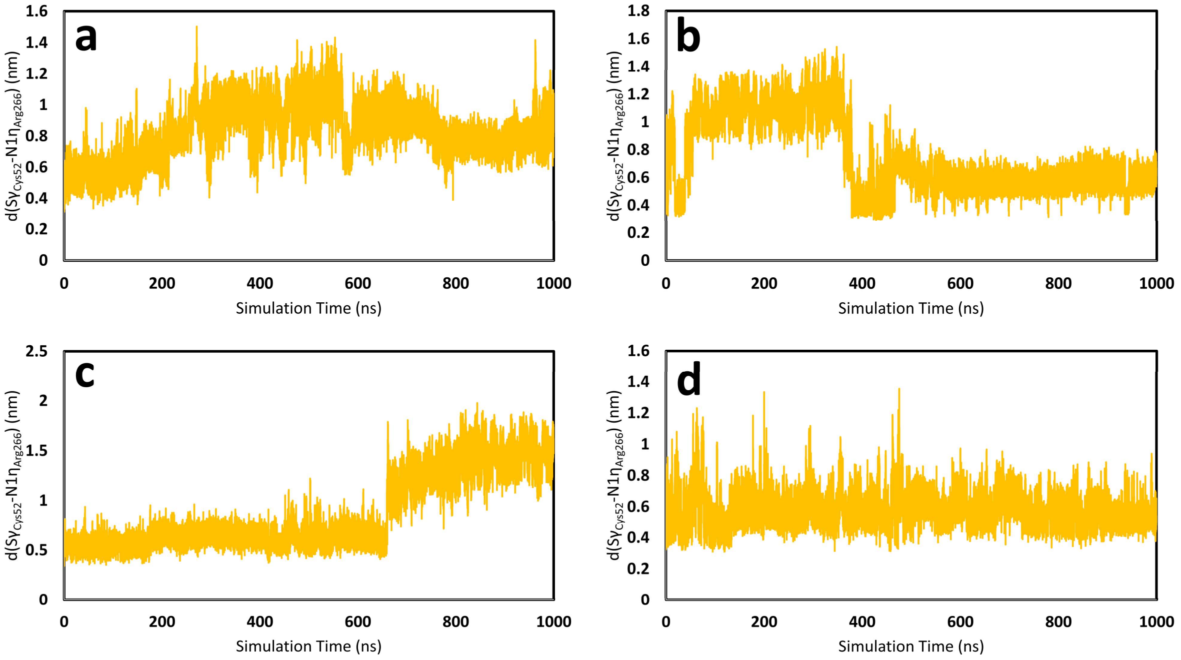

Figure S5: ***a.*** *variation of d(S*γ_{Cys52}*-N1*η_{Arg266}*) for chain A for the first 1000 ns simulation of* ***C****;* ***b.*** *variation of d(S*γ_{Cys52}*-N1*η_{Arg266}*) for chain B for the first 1000 ns simulation of* ***C****;* ***c.*** *variation of d(S*γ_{Cys52}*-N1*η_{Arg266}*) for chain A for the second 1000 ns simulation of* ***C****;* ***d.*** *variation of d(S*γ_{Cys52}*-N1*η_{Arg266}*) for chain B for the second 1000 ns simulation of* ***C****.*

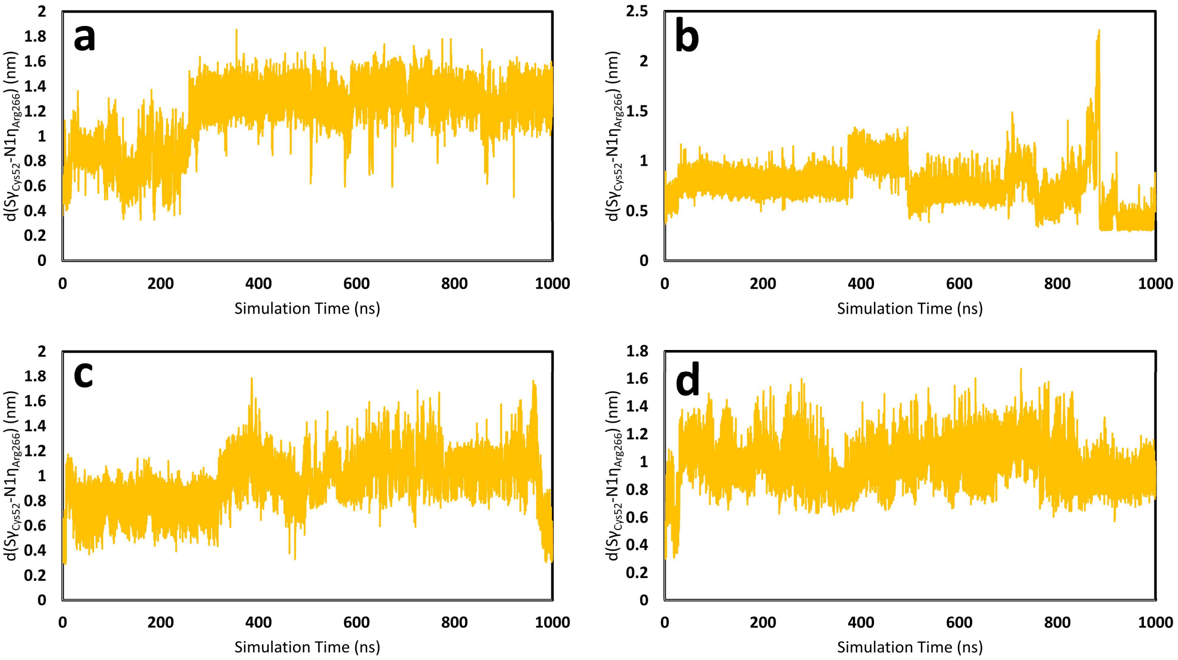

***Figure S6: a.** variation of $d(S\gamma_{Cys52}\text{-}N1\eta_{Arg266})$ for chain A for the first 1000 ns simulation of **E**; **b.** variation of $d(S\gamma_{Cys52}\text{-}N1\eta_{Arg266})$ for chain B for the first 1000 ns simulation of **E**; **c.** variation of $d(S\gamma_{Cys52}\text{-}N1\eta_{Arg266})$ for chain A for the second 1000 ns simulation of **E**; **d.** variation of $d(S\gamma_{Cys52}\text{-}N1\eta_{Arg266})$ for chain B for the second 1000 ns simulation of **E**.*

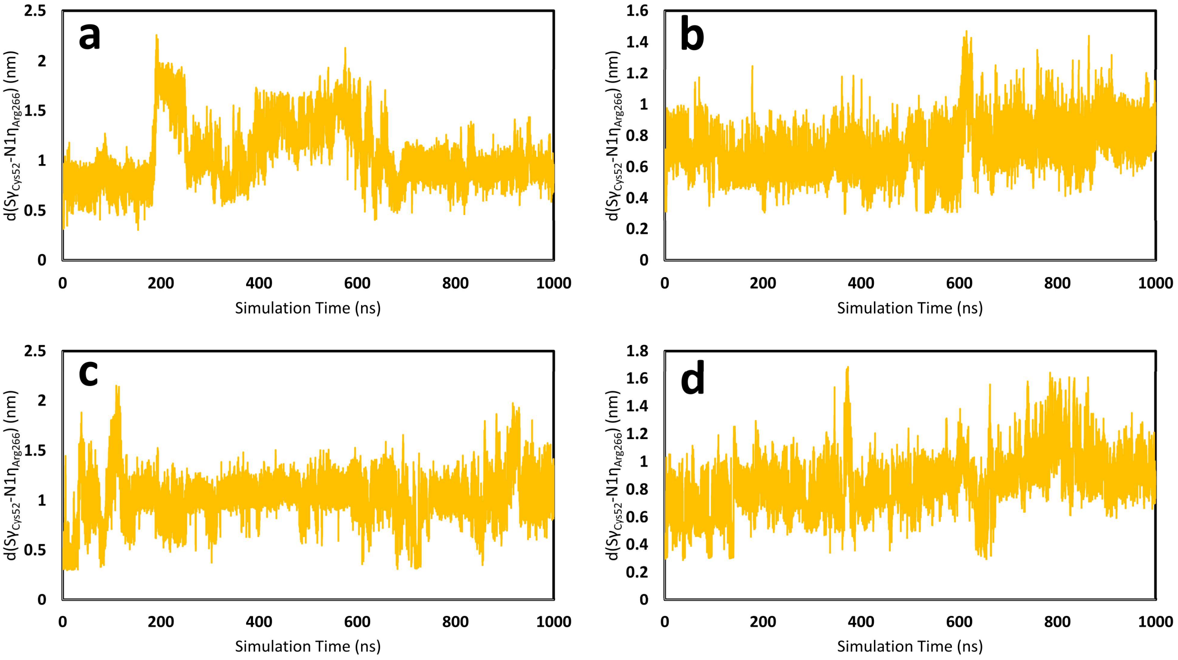

***Figure S7: a.** variation of $d(S\gamma_{Cys52}\text{-}N1\eta_{Arg266})$ for chain A for the first 1000 ns simulation of **F**; **b.** variation of $d(S\gamma_{Cys52}\text{-}N1\eta_{Arg266})$ for chain B for the first 1000 ns simulation of **F**; **c.** variation of $d(S\gamma_{Cys52}\text{-}N1\eta_{Arg266})$ for chain A for the second 1000 ns simulation of **F**; **d.** variation of $d(S\gamma_{Cys52}\text{-}N1\eta_{Arg266})$ for chain B for the second 1000 ns simulation of **F**.*

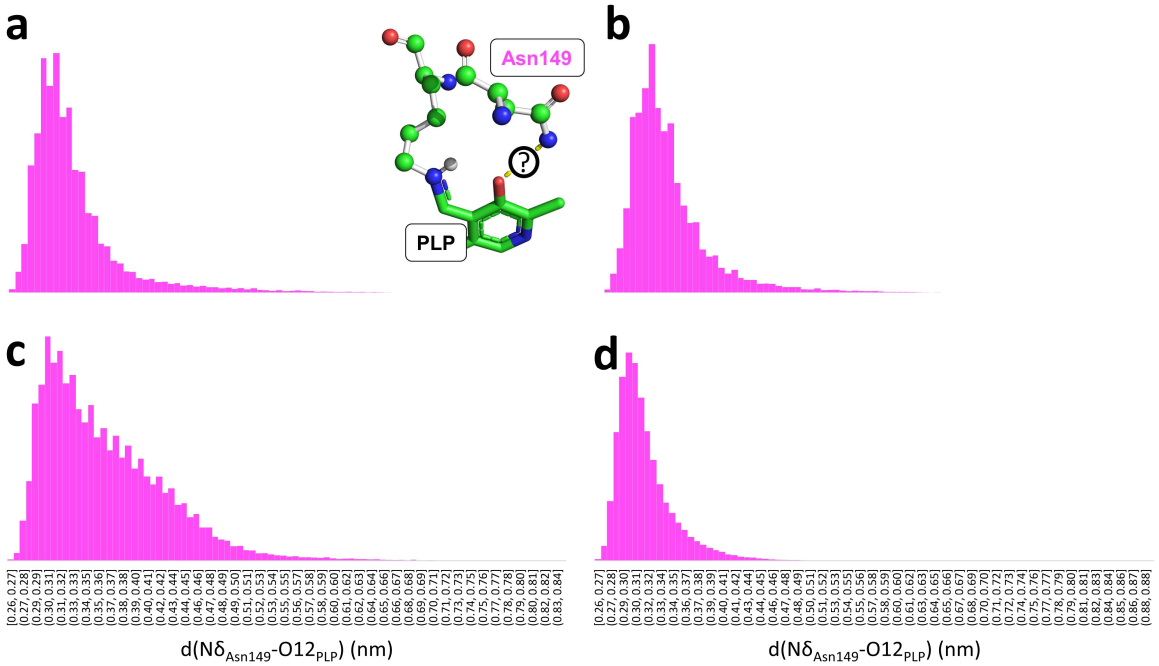

Figure S8:* *a. *histogram of d(Nδ$_{Asn149}$-O12$_{PLP}$) for chain A for the first 1000 ns simulation of **A**;* ***b.*** *histogram of d(Nδ$_{Asn149}$-O12$_{PLP}$) for chain B for the first 1000 ns simulation of **A**;* ***c.*** *histogram of d(Nδ$_{Asn149}$-O12$_{PLP}$) for chain A for the second 1000 ns simulation of **A**;* ***d.*** *histogram of d(Nδ$_{Asn149}$-O12$_{PLP}$) for chain B for the second 1000 ns simulation of **A**. The figure inset visually shows d(Nδ$_{Asn149}$-O12$_{PLP}$) and how it relates to PLP and Asn149 in human CBS.*

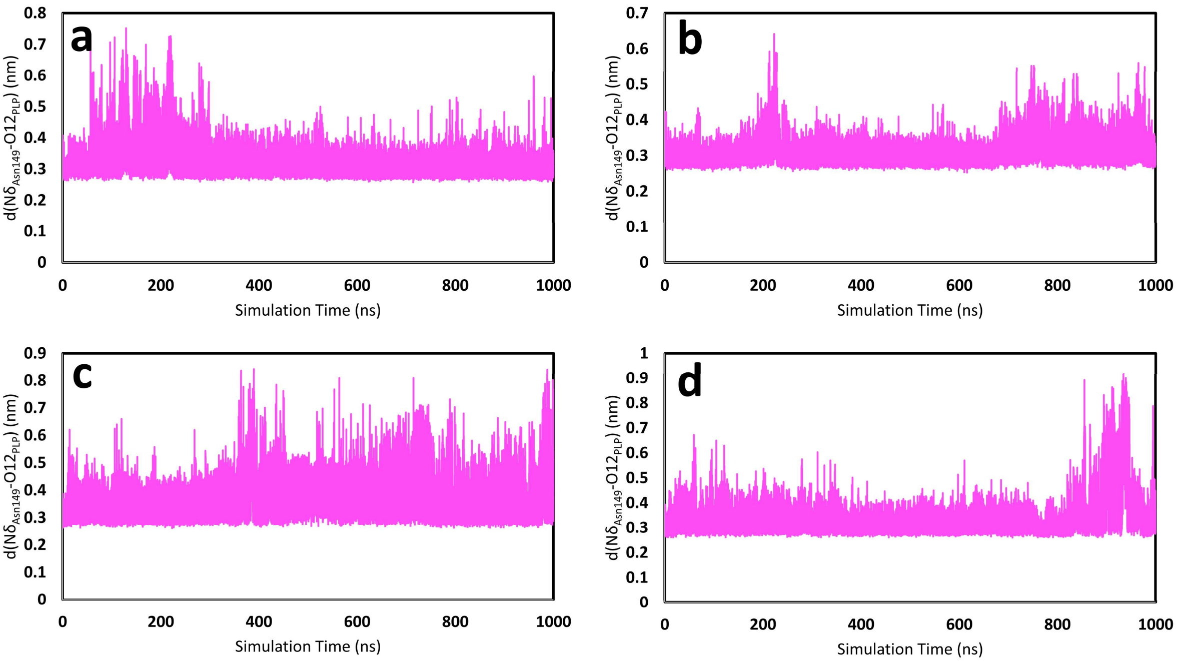

Figure S9:* *a. *variation of d(Nδ$_{Asn149}$-O12$_{PLP}$) for chain A for the first 1000 ns simulation of **A**;* ***b.*** *variation of d(Nδ$_{Asn149}$-O12$_{PLP}$) for chain B for the first 1000 ns simulation of **A**;* ***c.*** *variation of d(Nδ$_{Asn149}$-O12$_{PLP}$) for chain A for the second 1000 ns simulation of **A**;* ***d.*** *variation of d(Nδ$_{Asn149}$-O12$_{PLP}$) for chain B for the second 1000 ns simulation of **A**.*

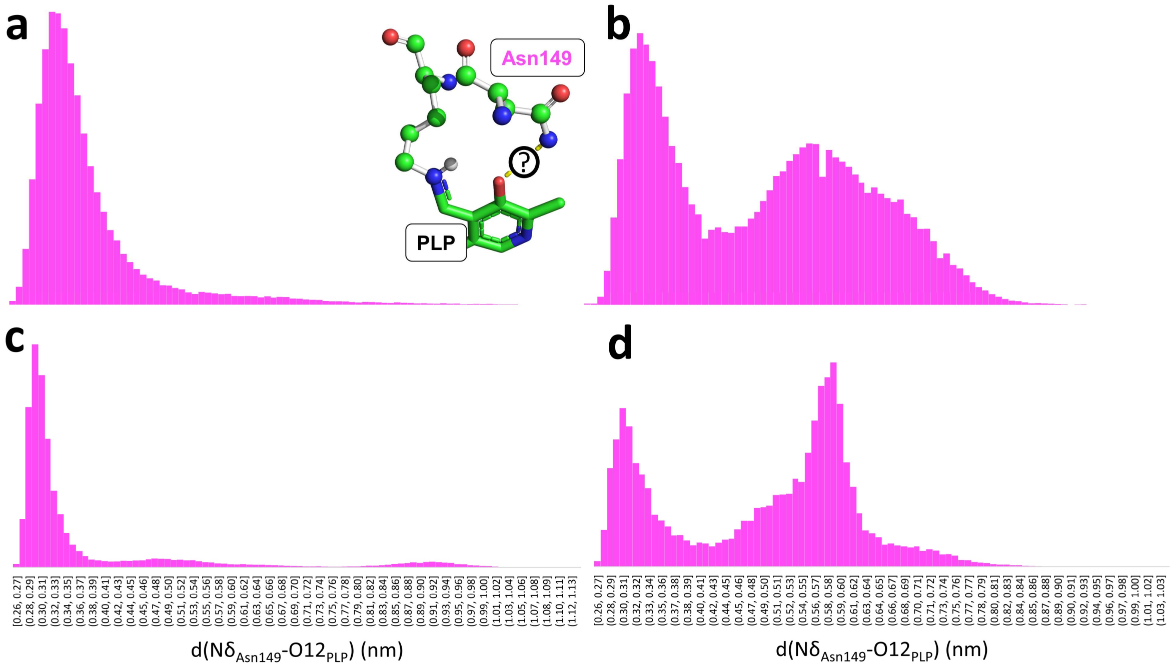

Figure S10: a. *histogram of d(Nδ$_{Asn149}$-O12$_{PLP}$) for chain A for the first 1000 ns simulation of **C**; **b.** histogram of d(Nδ$_{Asn149}$-O12$_{PLP}$) for chain B for the first 1000 ns simulation of **C**; **c.** histogram of d(Nδ$_{Asn149}$-O12$_{PLP}$) for chain A for the second 1000 ns simulation of **C**; **d.** histogram of d(Nδ$_{Asn149}$-O12$_{PLP}$) for chain B for the second 1000 ns simulation of **C**. The figure inset visually shows d(Nδ$_{Asn149}$-O12$_{PLP}$) and how it relates to PLP and Asn149 in human CBS.*

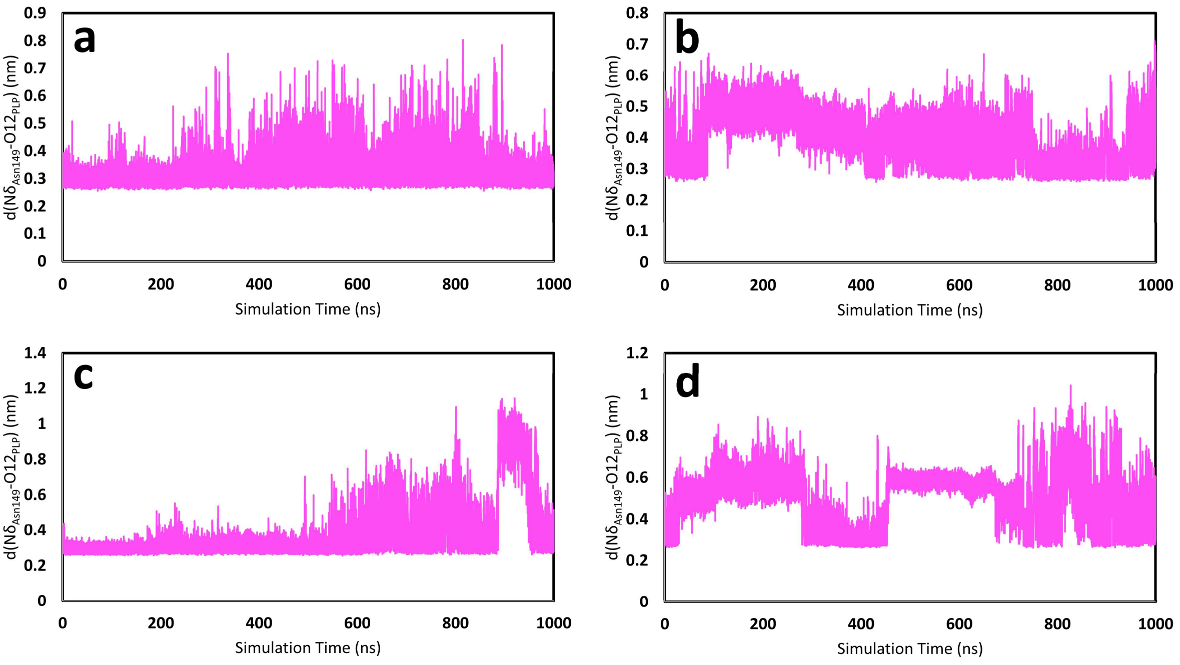

Figure S11: a. *variation of d(Nδ$_{Asn149}$-O12$_{PLP}$) for chain A for the first 1000 ns simulation of **C**; **b.** variation of d(Nδ$_{Asn149}$-O12$_{PLP}$) for chain B for the first 1000 ns simulation of **C**; **c.** variation of d(Nδ$_{Asn149}$-O12$_{PLP}$) for chain A for the second 1000 ns simulation of **C**; **d.** variation of d(Nδ$_{Asn149}$-O12$_{PLP}$) for chain B for the second 1000 ns simulation of **C**.*

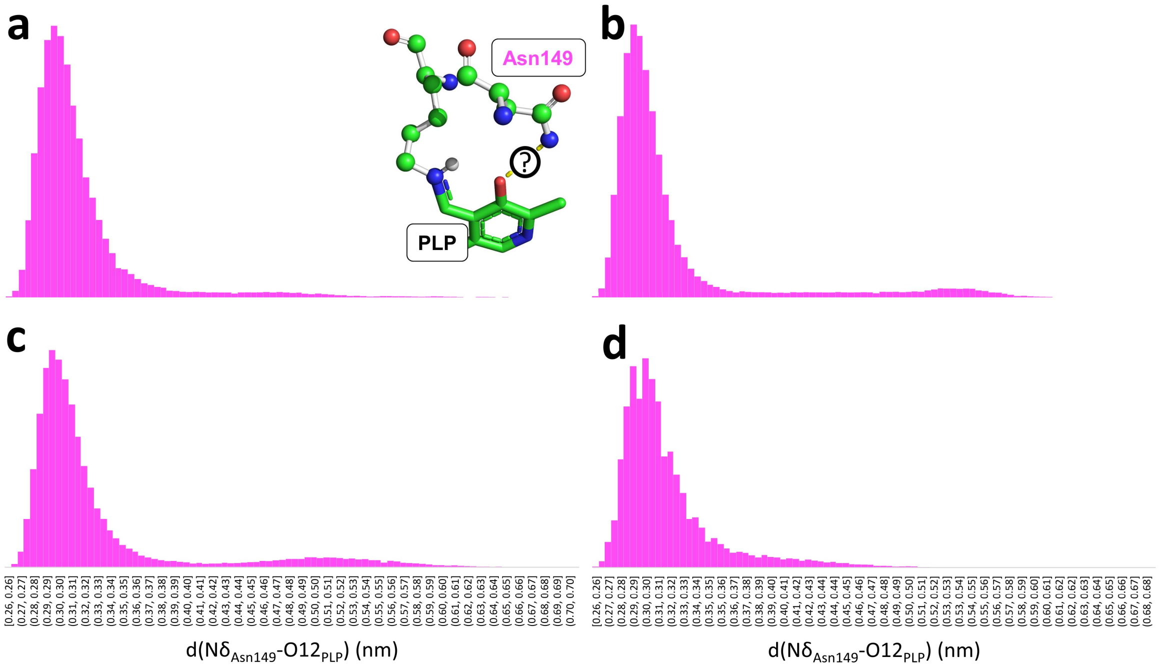

Figure S12:** a.* *histogram of* $d(N\delta_{Asn149}\text{-}O12_{PLP})$ *for chain A for the first 1000 ns simulation of* ***E**; **b. *histogram of* $d(N\delta_{Asn149}\text{-}O12_{PLP})$ *for chain B for the first 1000 ns simulation of* ***E**; **c.*** *histogram of* $d(N\delta_{Asn149}\text{-}O12_{PLP})$ *for chain A for the second 1000 ns simulation of* ***E**; **d.*** *histogram of* $d(N\delta_{Asn149}\text{-}O12_{PLP})$ *for chain B for the second 1000 ns simulation of* ***E**. The figure inset visually shows* $d(N\delta_{Asn149}\text{-}O12_{PLP})$ *and how it relates to PLP and Asn149 in human CBS.*

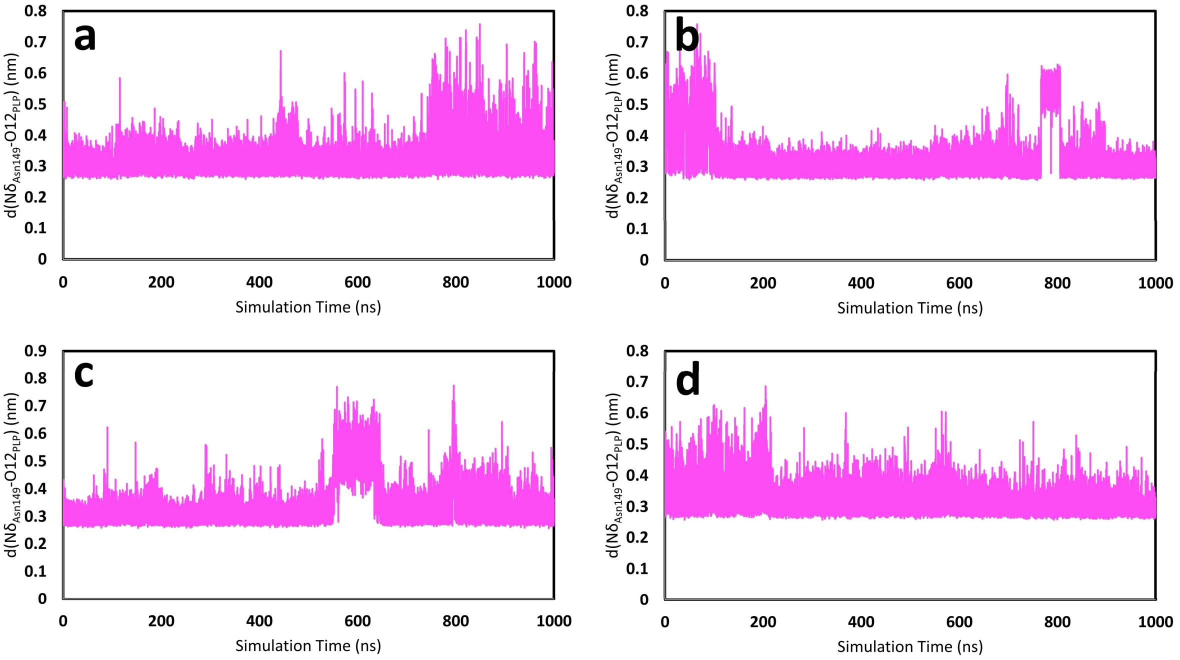

Figure S13:** a.* *variation of* $d(N\delta_{Asn149}\text{-}O12_{PLP})$ *for chain A for the first 1000 ns simulation of* ***E**; **b. *variation of* $d(N\delta_{Asn149}\text{-}O12_{PLP})$ *for chain B for the first 1000 ns simulation of* ***E**; **c.*** *variation of* $d(N\delta_{Asn149}\text{-}O12_{PLP})$ *for chain A for the second 1000 ns simulation of* ***E**; **d.*** *variation of* $d(N\delta_{Asn149}\text{-}O12_{PLP})$ *for chain B for the second 1000 ns simulation of* ***E**.*

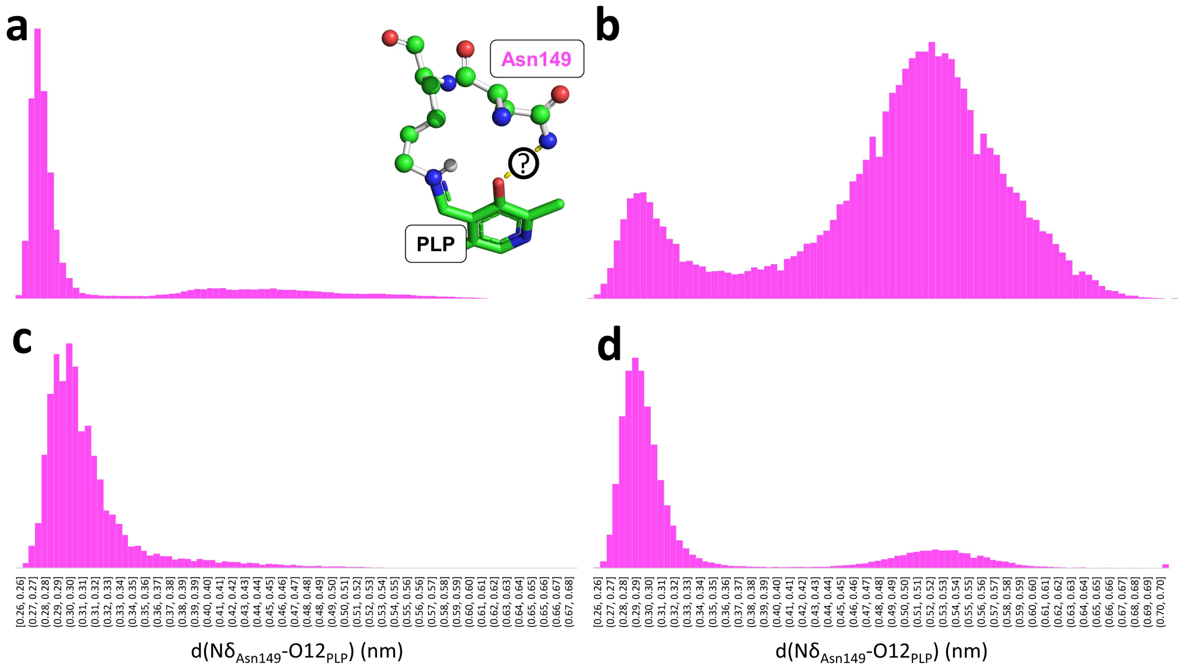

Figure S14: ***a.*** *histogram of d(Nδ_{Asn149}-O12$_{PLP}$) for chain A for the first 1000 ns simulation of* ***F****;* ***b.*** *histogram of d(Nδ_{Asn149}-O12$_{PLP}$) for chain B for the first 1000 ns simulation of* ***F****;* ***c.*** *histogram of d(Nδ_{Asn149}-O12$_{PLP}$) for chain A for the second 1000 ns simulation of* ***F****;* ***d.*** *histogram of d(Nδ_{Asn149}-O12$_{PLP}$) for chain B for the second 1000 ns simulation of* ***F****. The figure inset visually shows d(Nδ_{Asn149}-O12$_{PLP}$) and how it relates to PLP and Asn149 in human CBS.*

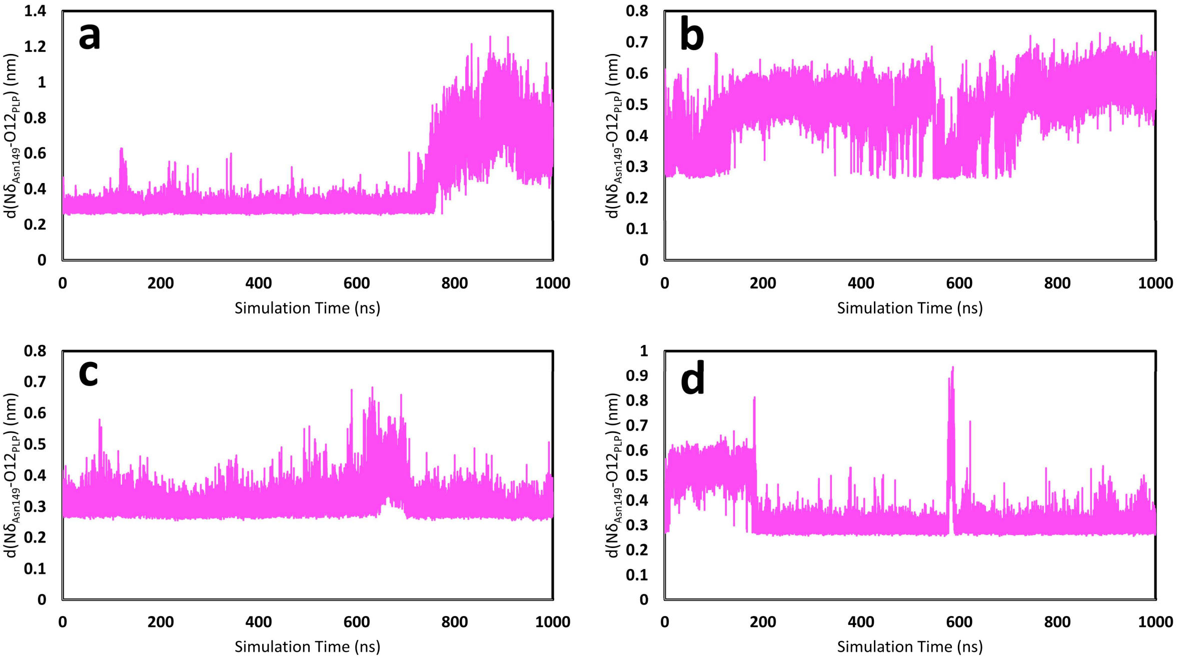

Figure S15: ***a.*** *variation of d(Nδ_{Asn149}-O12$_{PLP}$) for chain A for the first 1000 ns simulation of* ***F****;* ***b.*** *variation of d(Nδ_{Asn149}-O12$_{PLP}$) for chain B for the first 1000 ns simulation of* ***F****;* ***c.*** *variation of d(Nδ_{Asn149}-O12$_{PLP}$) for chain A for the second 1000 ns simulation of* ***F****;* ***d.*** *variation of d(Nδ_{Asn149}-O12$_{PLP}$) for chain B for the second 1000 ns simulation of* ***F****.*

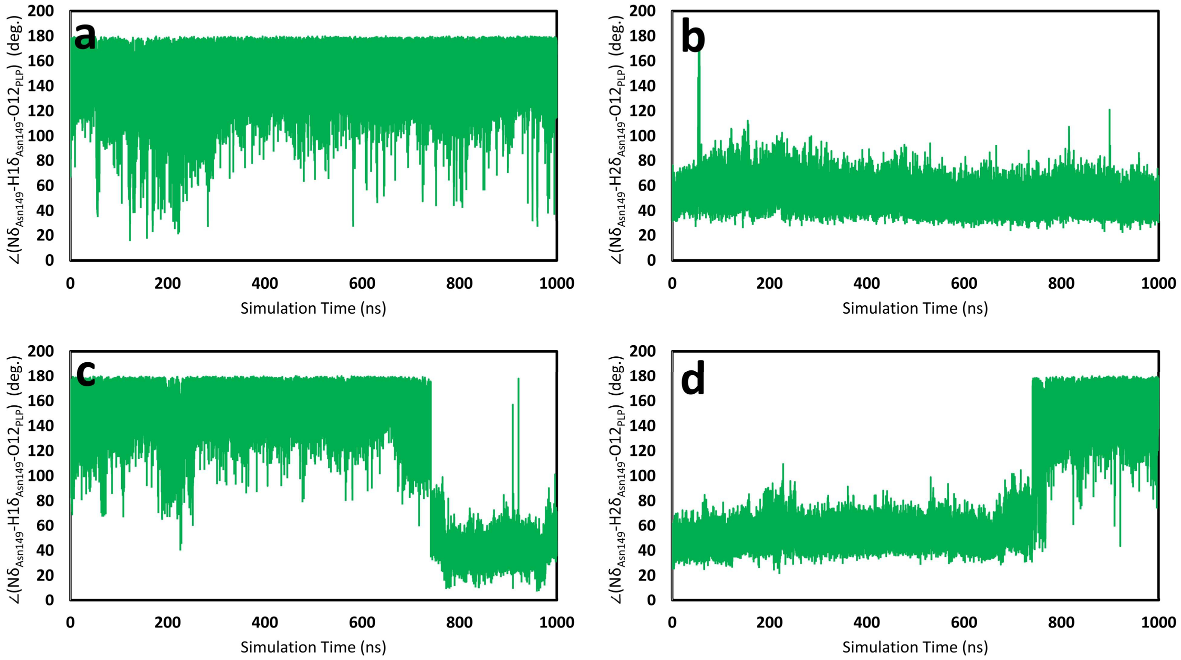

Figure S16:* *a. *variation of* $\angle(N\delta_{Asn149}\text{-}H1\delta_{Asn149}\text{-}O12_{PLP})$ *for chain A for the first 1000 ns simulation of* ***A****;* ***b.*** *variation of* $\angle(N\delta_{Asn149}\text{-}H2\delta_{Asn149}\text{-}O12_{PLP})$ *for chain A for the first 1000 ns simulation of* ***A****;* ***c.*** *variation of* $\angle(N\delta_{Asn149}\text{-}H1\delta_{Asn149}\text{-}O12_{PLP})$ *for chain B for the first 1000 ns simulation of* ***A****;* ***d.*** *variation of* $\angle(N\delta_{Asn149}\text{-}H2\delta_{Asn149}\text{-}O12_{PLP})$ *for chain B for the first 1000 ns simulation of* ***A****.*

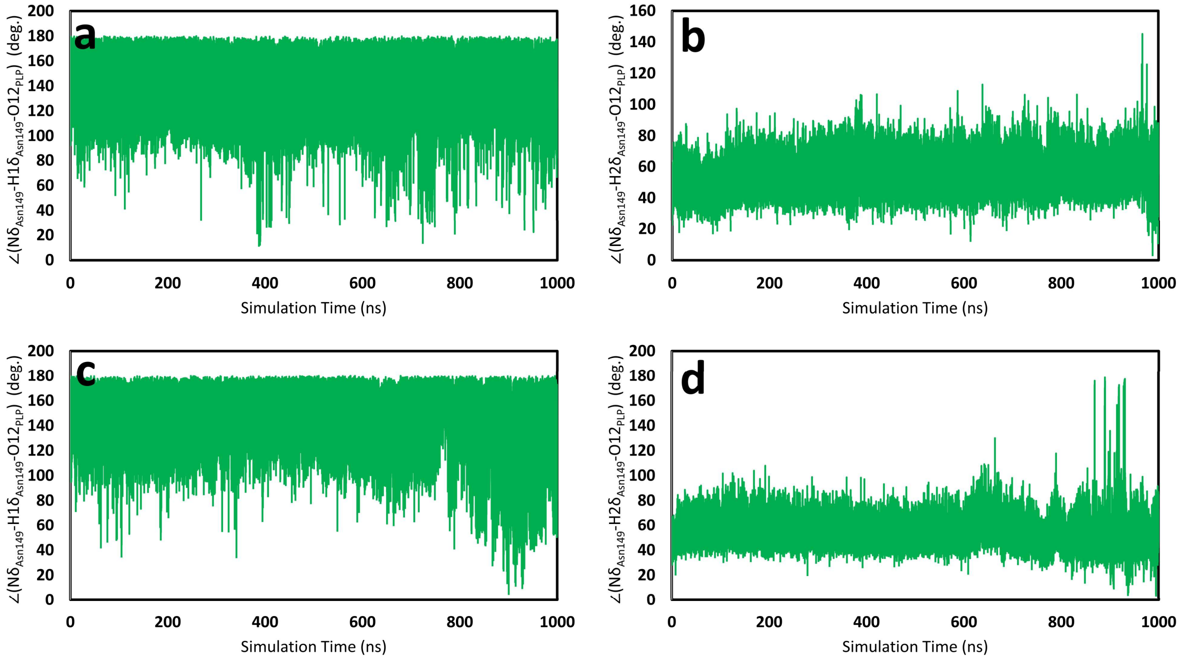

Figure S17:* *a. *variation of* $\angle(N\delta_{Asn149}\text{-}H1\delta_{Asn149}\text{-}O12_{PLP})$ *for chain A for the second 1000 ns simulation of* ***A****;* ***b.*** *variation of* $\angle(N\delta_{Asn149}\text{-}H2\delta_{Asn149}\text{-}O12_{PLP})$ *for chain A for the second 1000 ns simulation of* ***A****;* ***c.*** *variation of* $\angle(N\delta_{Asn149}\text{-}H1\delta_{Asn149}\text{-}O12_{PLP})$ *for chain B for the second 1000 ns simulation of* ***A****;* ***d.*** *variation of* $\angle(N\delta_{Asn149}\text{-}H2\delta_{Asn149}\text{-}O12_{PLP})$ *for chain B for the second 1000 ns simulation of* ***A****.*

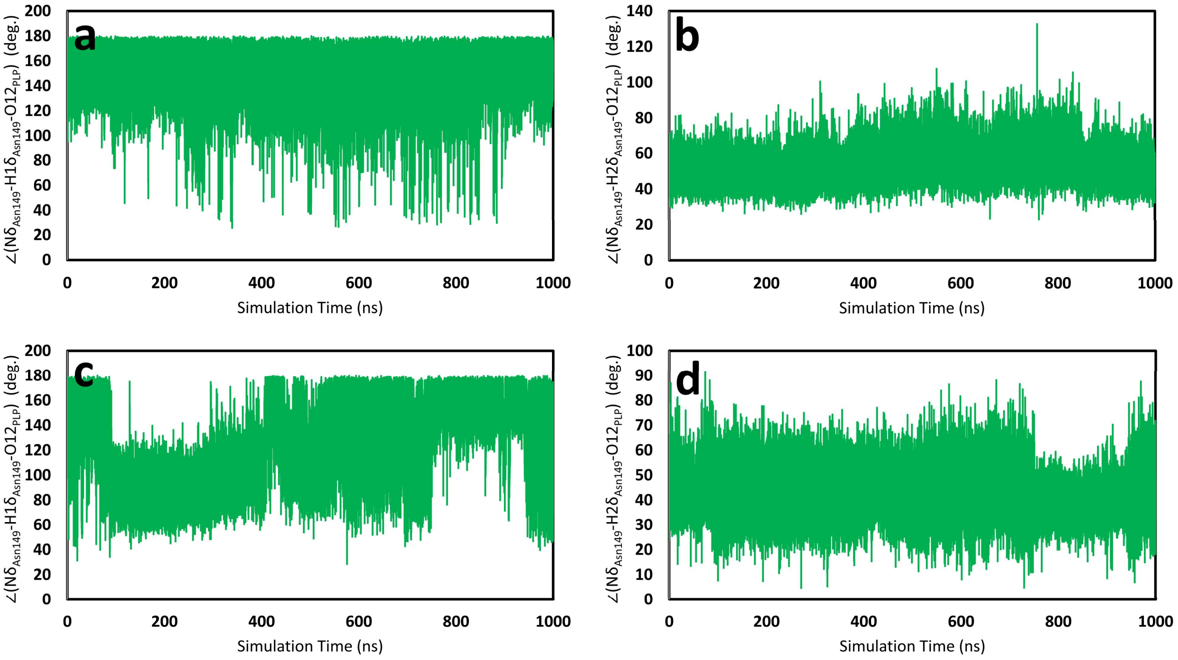

Figure S18: ***a.*** *variation of* $\angle(N\delta_{Asn149}\text{-}H1\delta_{Asn149}\text{-}O12_{PLP})$ *for chain A for the first 1000 ns simulation of* ***C****;* ***b.*** *variation of* $\angle(N\delta_{Asn149}\text{-}H2\delta_{Asn149}\text{-}O12_{PLP})$ *for chain A for the first 1000 ns simulation of* ***C****;* ***c.*** *variation of* $\angle(N\delta_{Asn149}\text{-}H1\delta_{Asn149}\text{-}O12_{PLP})$ *for chain B for the first 1000 ns simulation of* ***C****;* ***d.*** *variation of* $\angle(N\delta_{Asn149}\text{-}H2\delta_{Asn149}\text{-}O12_{PLP})$ *for chain B for the first 1000 ns simulation of* ***C****.*

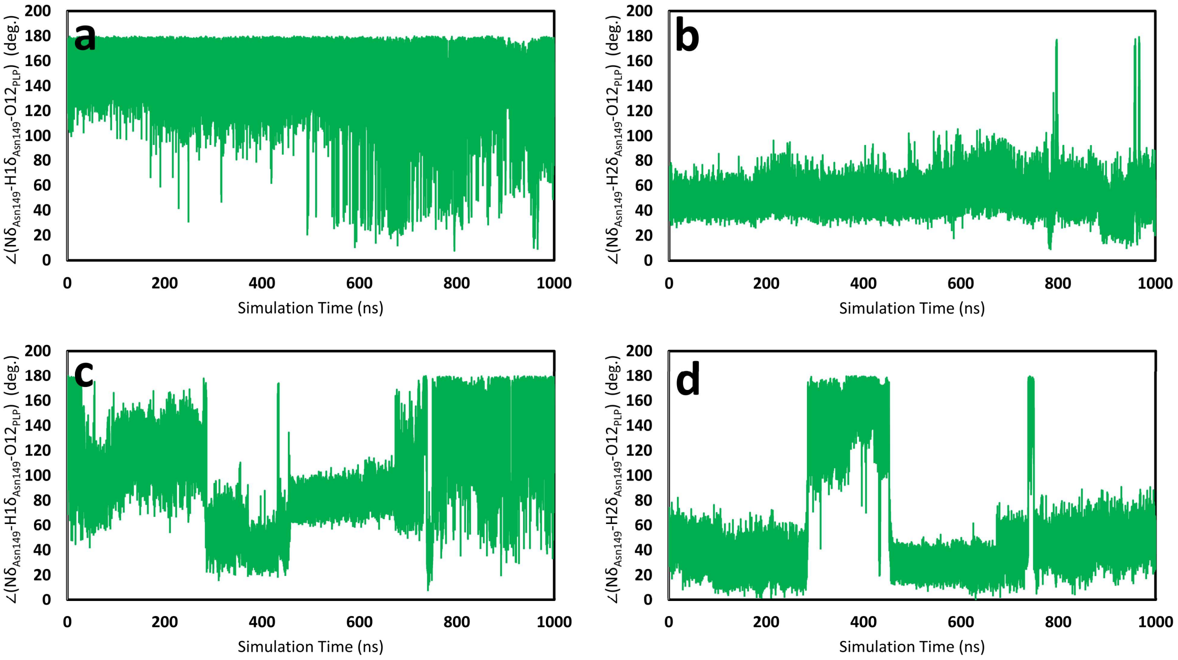

Figure S19: ***a.*** *variation of* $\angle(N\delta_{Asn149}\text{-}H1\delta_{Asn149}\text{-}O12_{PLP})$ *for chain A for the second 1000 ns simulation of* ***C****;* ***b.*** *variation of* $\angle(N\delta_{Asn149}\text{-}H2\delta_{Asn149}\text{-}O12_{PLP})$ *for chain A for the second 1000 ns simulation of* ***C****;* ***c.*** *variation of* $\angle(N\delta_{Asn149}\text{-}H1\delta_{Asn149}\text{-}O12_{PLP})$ *for chain B for the second 1000 ns simulation of* ***C****;* ***d.*** *variation of* $\angle(N\delta_{Asn149}\text{-}H2\delta_{Asn149}\text{-}O12_{PLP})$ *for chain B for the second 1000 ns simulation of* ***C****.*

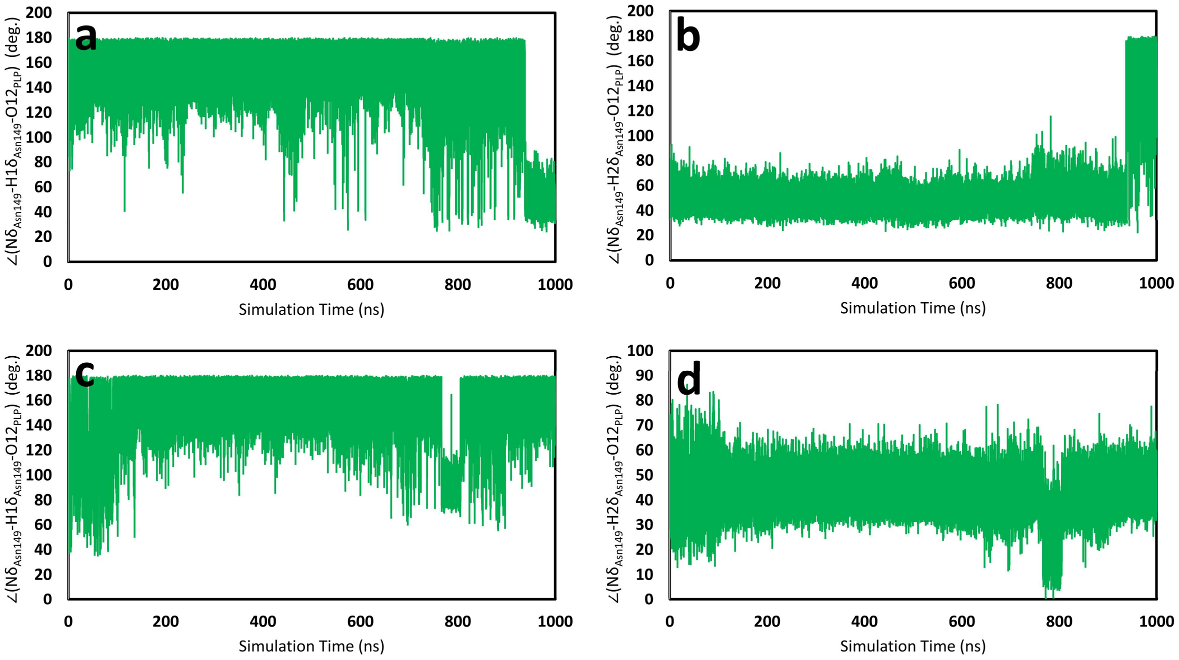

Figure S20: ***a.*** *variation of* $\angle(N\delta_{Asn149}\text{-}H1\delta_{Asn149}\text{-}O12_{PLP})$ *for chain A for the first 1000 ns simulation of* ***E***; ***b.*** *variation of* $\angle(N\delta_{Asn149}\text{-}H2\delta_{Asn149}\text{-}O12_{PLP})$ *for chain A for the first 1000 ns simulation of* ***E***; ***c.*** *variation of* $\angle(N\delta_{Asn149}\text{-}H1\delta_{Asn149}\text{-}O12_{PLP})$ *for chain B for the first 1000 ns simulation of* ***E***; ***d.*** *variation of* $\angle(N\delta_{Asn149}\text{-}H2\delta_{Asn149}\text{-}O12_{PLP})$ *for chain B for the first 1000 ns simulation of* ***E***.

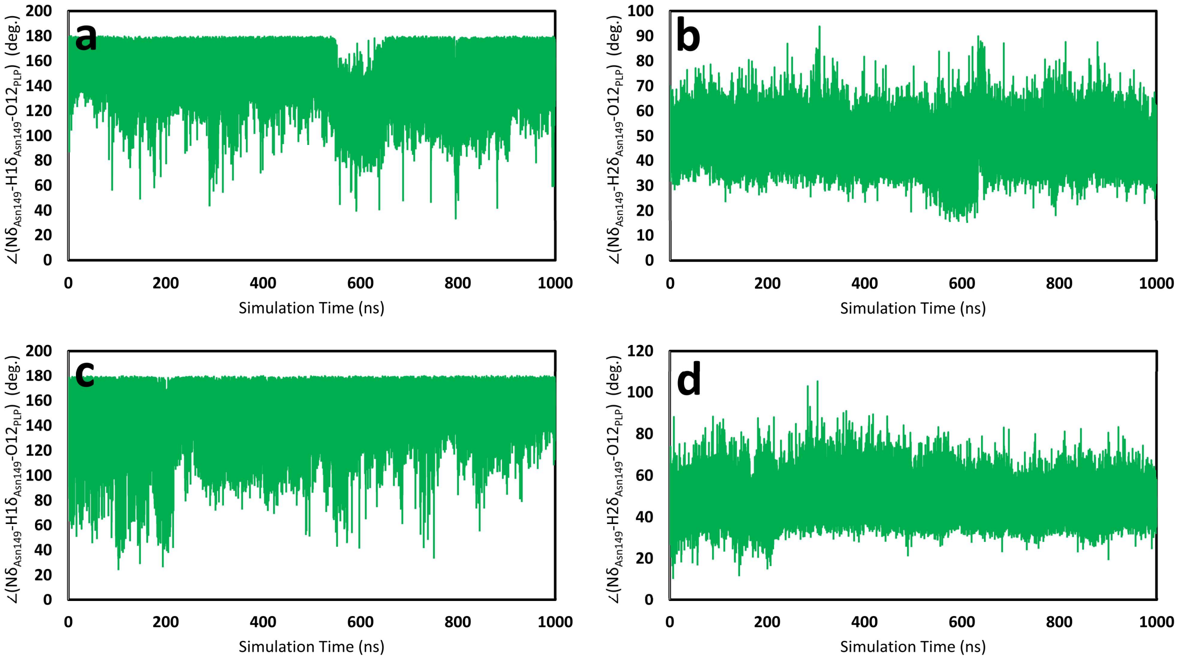

Figure S21: ***a.*** *variation of* $\angle(N\delta_{Asn149}\text{-}H1\delta_{Asn149}\text{-}O12_{PLP})$ *for chain A for the second 1000 ns simulation of* ***E***; ***b.*** *variation of* $\angle(N\delta_{Asn149}\text{-}H2\delta_{Asn149}\text{-}O12_{PLP})$ *for chain A for the second 1000 ns simulation of* ***E***; ***c.*** *variation of* $\angle(N\delta_{Asn149}\text{-}H1\delta_{Asn149}\text{-}O12_{PLP})$ *for chain B for the second 1000 ns simulation of* ***E***; ***d.*** *variation of* $\angle(N\delta_{Asn149}\text{-}H2\delta_{Asn149}\text{-}O12_{PLP})$ *for chain B for the second 1000 ns simulation of* ***E***.

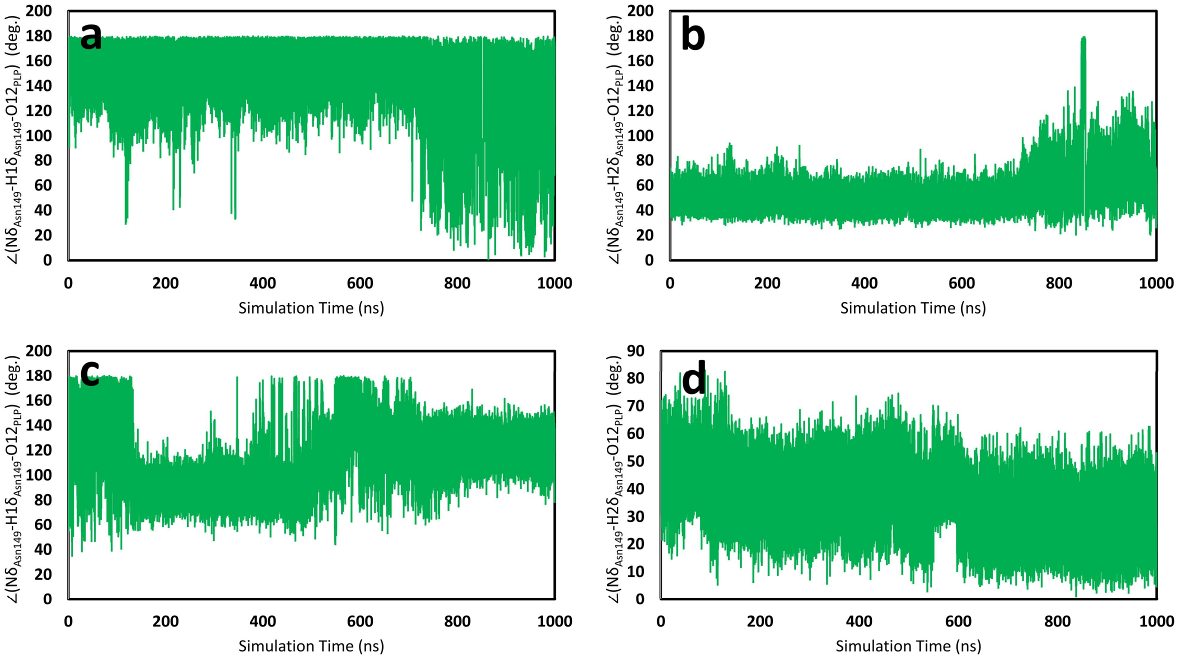

Figure S22: ***a.*** *variation of* $\angle(N\delta_{Asn149}\text{-}H1\delta_{Asn149}\text{-}O12_{PLP})$ *for chain A for the first 1000 ns simulation of* ***F****;* ***b.*** *variation of* $\angle(N\delta_{Asn149}\text{-}H2\delta_{Asn149}\text{-}O12_{PLP})$ *for chain A for the first 1000 ns simulation of* ***F****;* ***c.*** *variation of* $\angle(N\delta_{Asn149}\text{-}H1\delta_{Asn149}\text{-}O12_{PLP})$ *for chain B for the first 1000 ns simulation of* ***F****;* ***d.*** *variation of* $\angle(N\delta_{Asn149}\text{-}H2\delta_{Asn149}\text{-}O12_{PLP})$ *for chain B for the first 1000 ns simulation of* ***F****.*

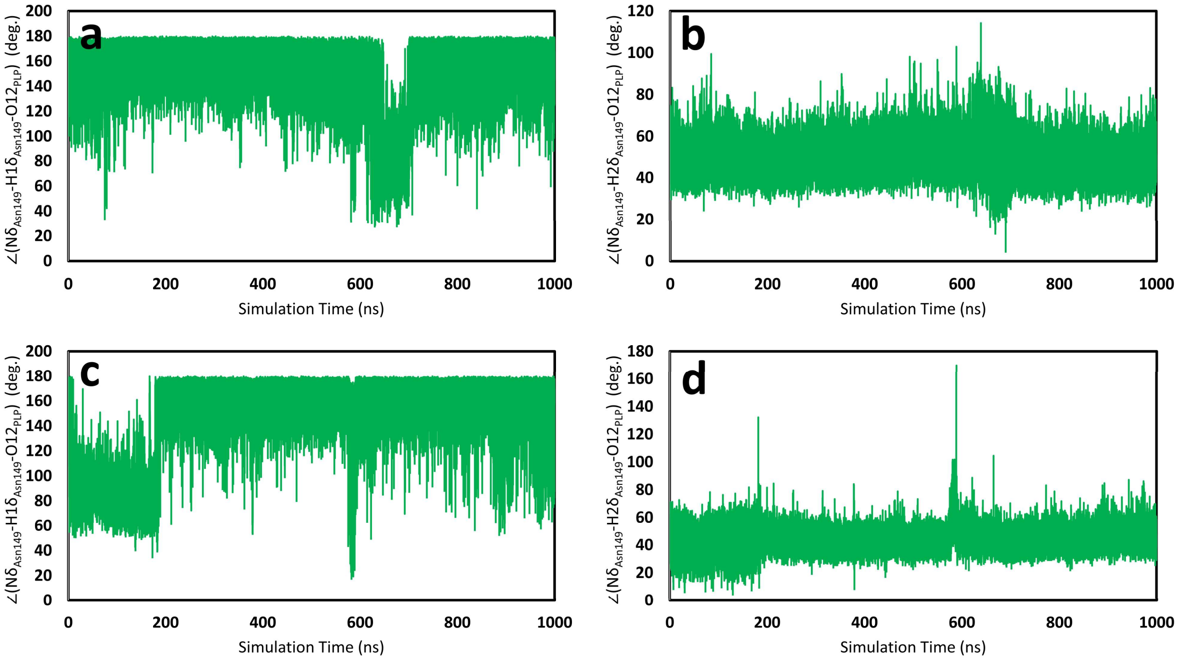

Figure S23: ***a.*** *variation of* $\angle(N\delta_{Asn149}\text{-}H1\delta_{Asn149}\text{-}O12_{PLP})$ *for chain A for the second 1000 ns simulation of* ***F****;* ***b.*** *variation of* $\angle(N\delta_{Asn149}\text{-}H2\delta_{Asn149}\text{-}O12_{PLP})$ *for chain A for the second 1000 ns simulation of* ***F****;* ***c.*** *variation of* $\angle(N\delta_{Asn149}\text{-}H1\delta_{Asn149}\text{-}O12_{PLP})$ *for chain B for the second 1000 ns simulation of* ***F****;* ***d.*** *variation of* $\angle(N\delta_{Asn149}\text{-}H2\delta_{Asn149}\text{-}O12_{PLP})$ *for chain B for the second 1000 ns simulation of* ***F****.*

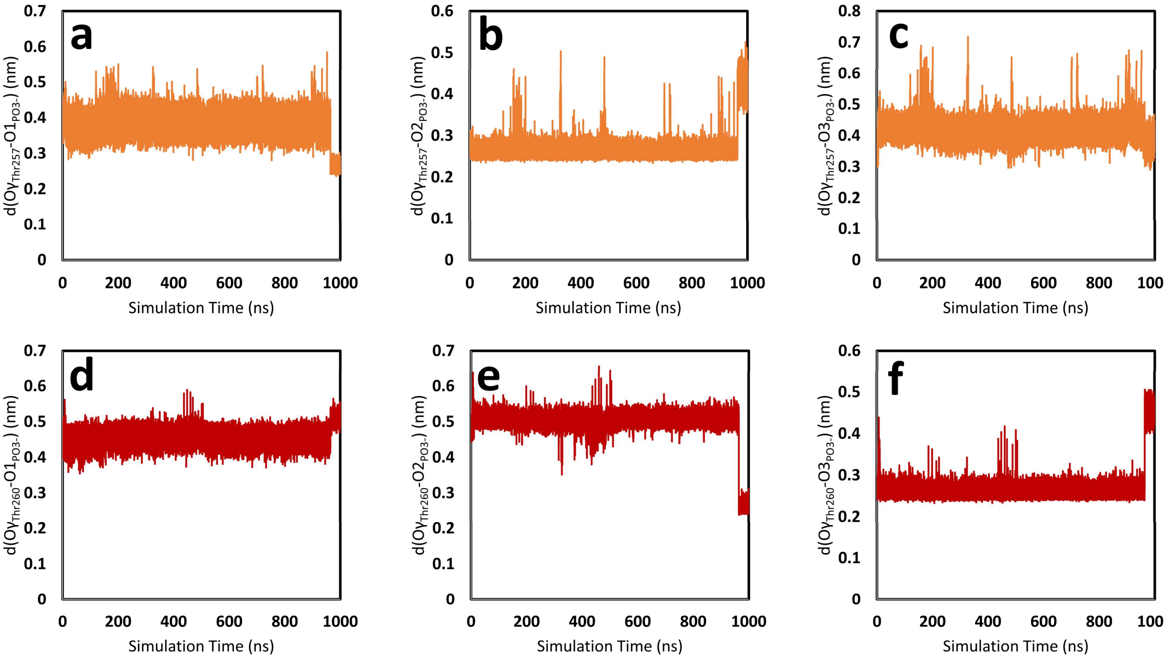

Figure S24: ***a,b,c.*** *variation of d(Oγ$_{Thr257}$-O1/2/3$_{PO3-}$) for chain A for the first 1000 ns simulation of* ***A****;* ***d,e,f.*** *variation of d(Oγ$_{Thr260}$-O1/2/3$_{PO3-}$) for chain A for the first 1000 ns simulation of* ***A****.*

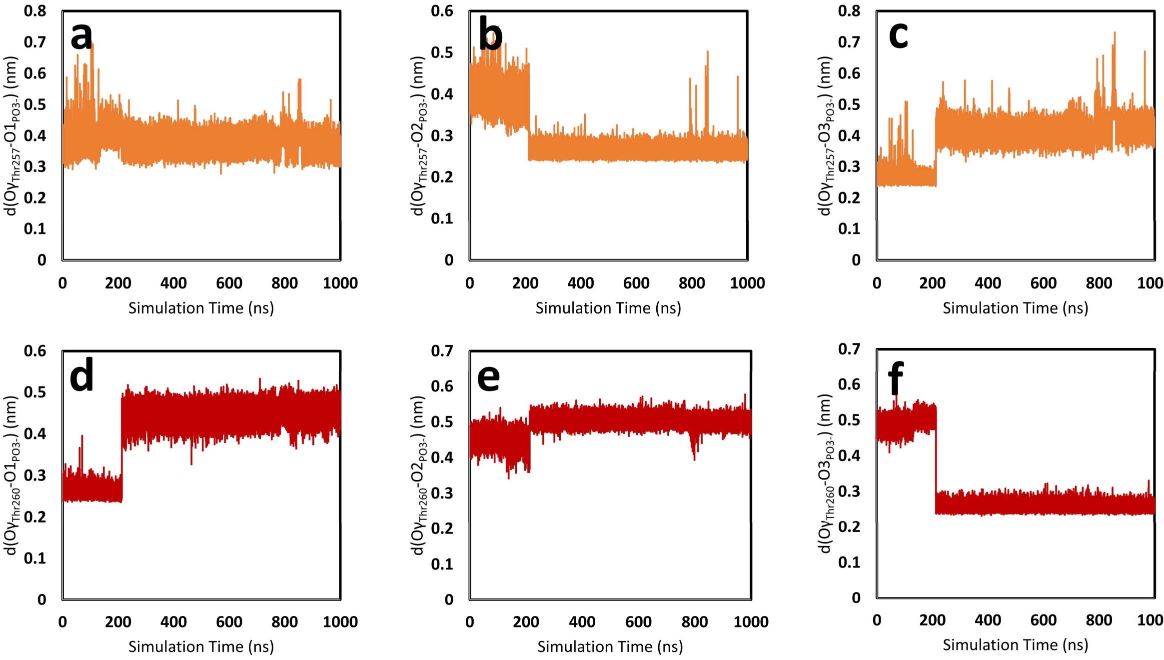

Figure S25: ***a,b,c.*** *variation of d(Oγ$_{Thr257}$-O1/2/3$_{PO3-}$) for chain B for the first 1000 ns simulation of* ***A****;* ***d,e,f.*** *variation of d(Oγ$_{Thr260}$-O1/2/3$_{PO3-}$) for chain B for the first 1000 ns simulation of* ***A****.*

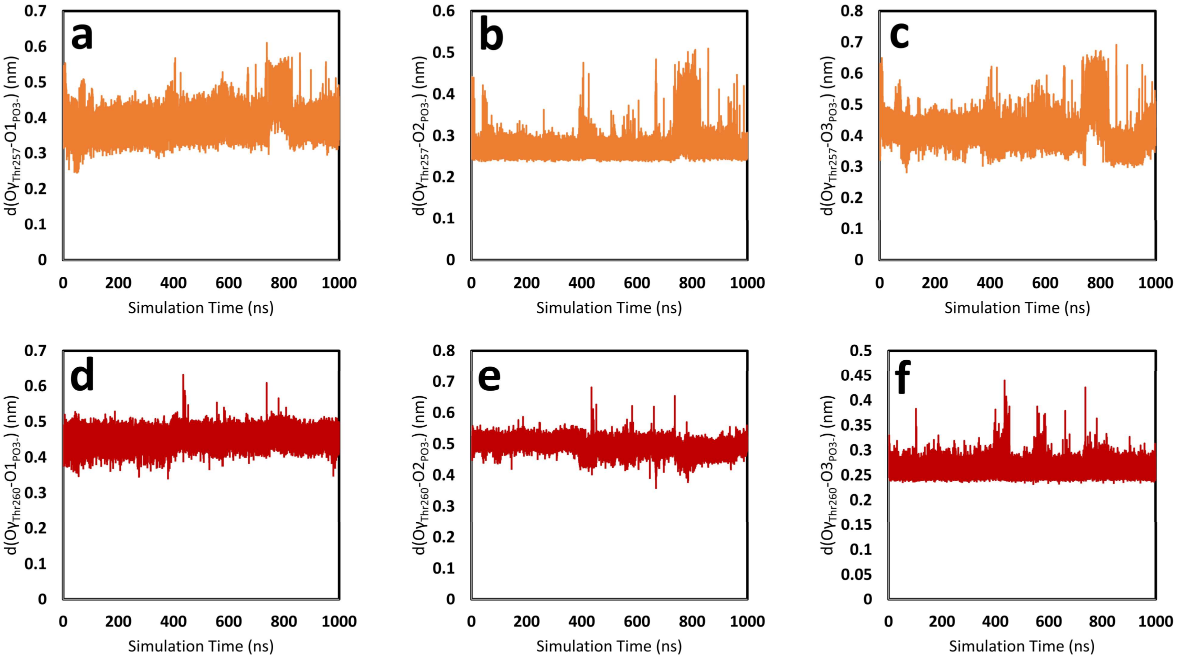

Figure S26:* *a,b,c. *variation of d(Oγ$_{Thr257}$-O1/2/3$_{PO3-}$) for chain A for the second 1000 ns simulation of **A**; **d,e,f.** variation of d(Oγ$_{Thr260}$-O1/2/3$_{PO3-}$) for chain A for the second 1000 ns simulation of **A**.*

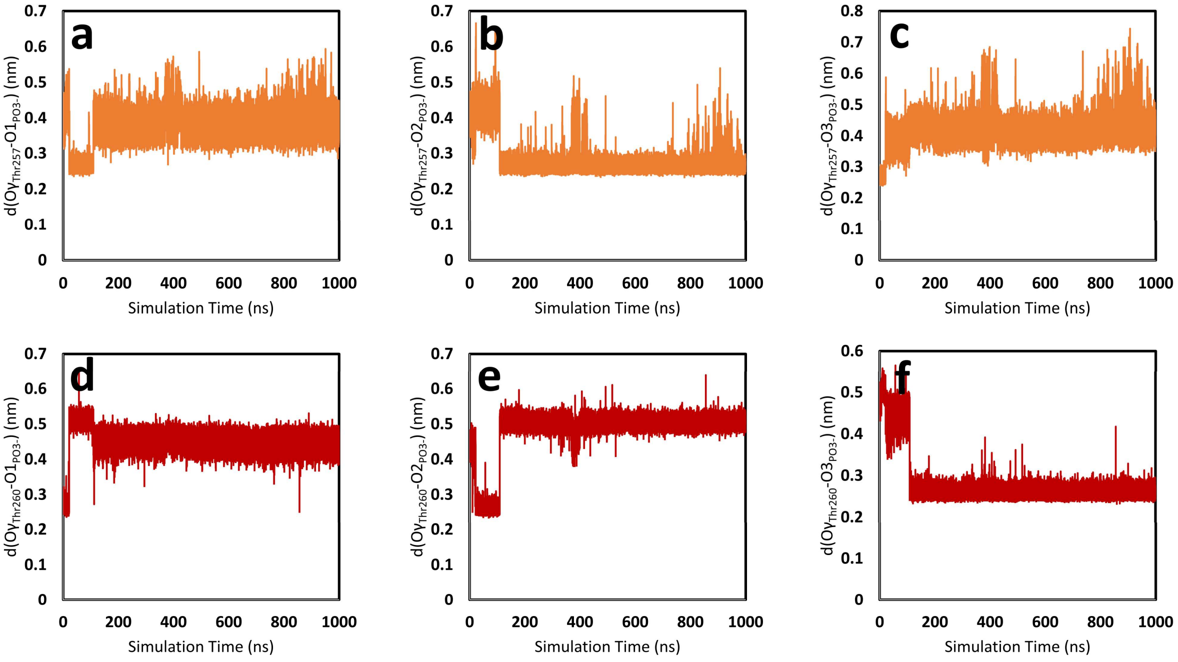

Figure S27:* *a,b,c. *variation of d(Oγ$_{Thr257}$-O1/2/3$_{PO3-}$) for chain B for the second 1000 ns simulation of **A**; **d,e,f.** variation of d(Oγ$_{Thr260}$-O1/2/3$_{PO3-}$) for chain B for the second 1000 ns simulation of **A**.*

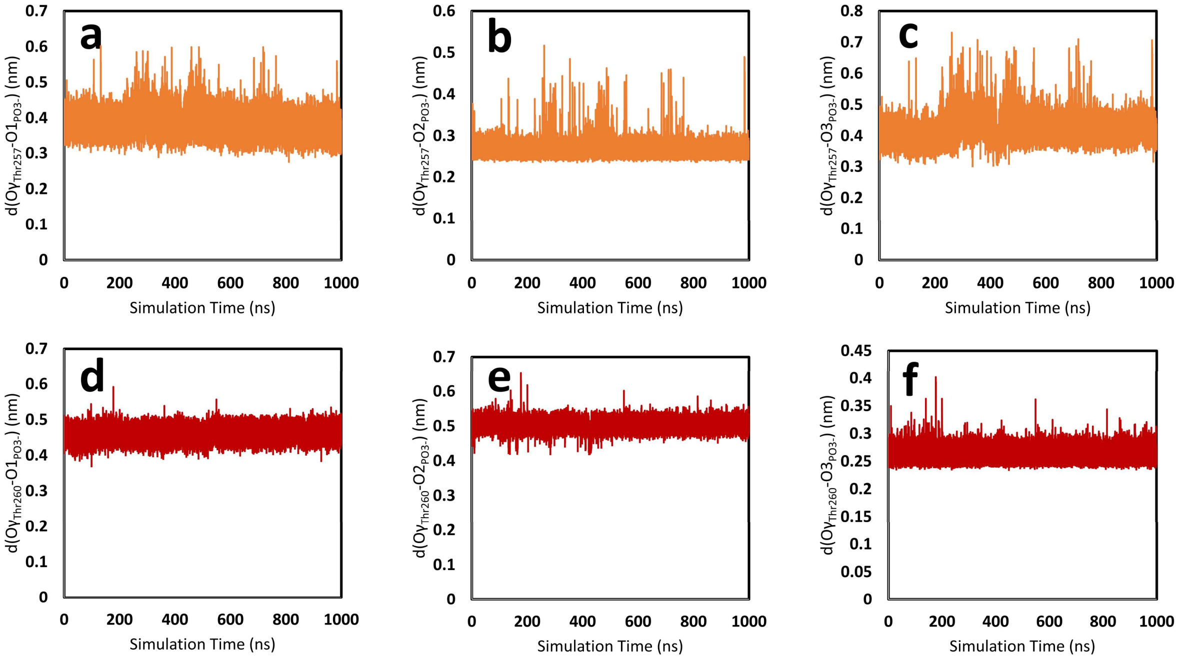

Figure S28: ***a,b,c.*** *variation of* $d(O\gamma_{Thr257}\text{-}O1/2/3_{PO3-})$ *for chain A for the first 1000 ns simulation of* ***C****;* ***d,e,f.*** *variation of* $d(O\gamma_{Thr260}\text{-}O1/2/3_{PO3-})$ *for chain A for the first 1000 ns simulation of* ***C****.*

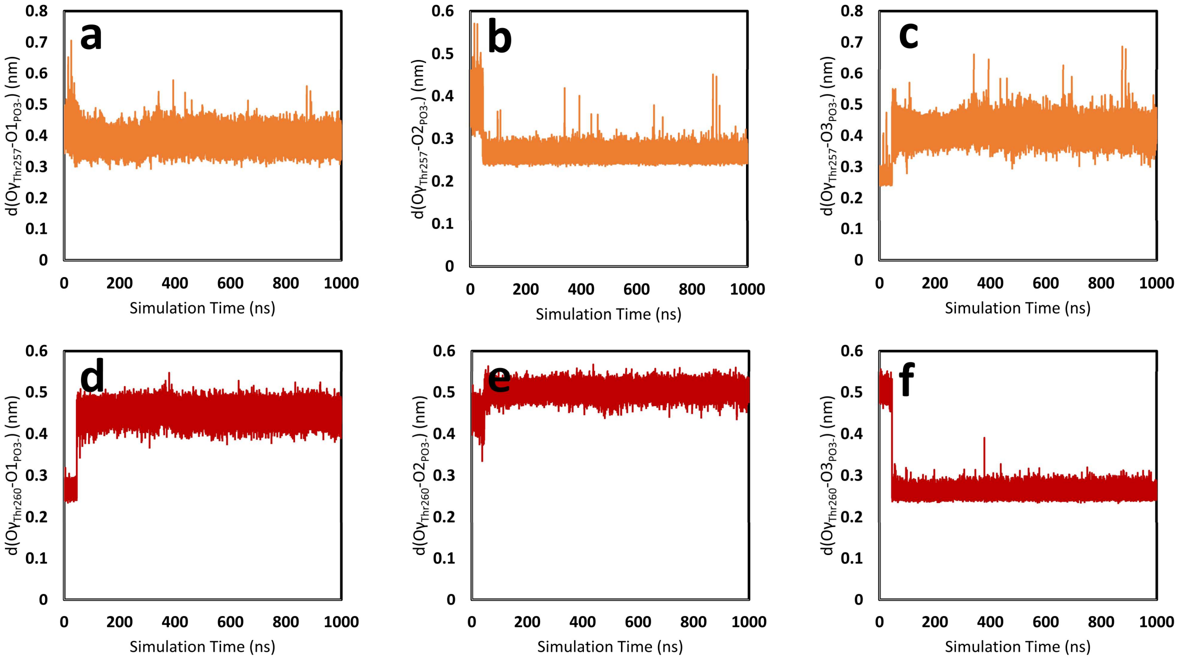

Figure S29: ***a,b,c.*** *variation of* $d(O\gamma_{Thr257}\text{-}O1/2/3_{PO3-})$ *for chain B for the first 1000 ns simulation of* ***C****;* ***d,e,f.*** *variation of* $d(O\gamma_{Thr260}\text{-}O1/2/3_{PO3-})$ *for chain B for the first 1000 ns simulation of* ***C****.*

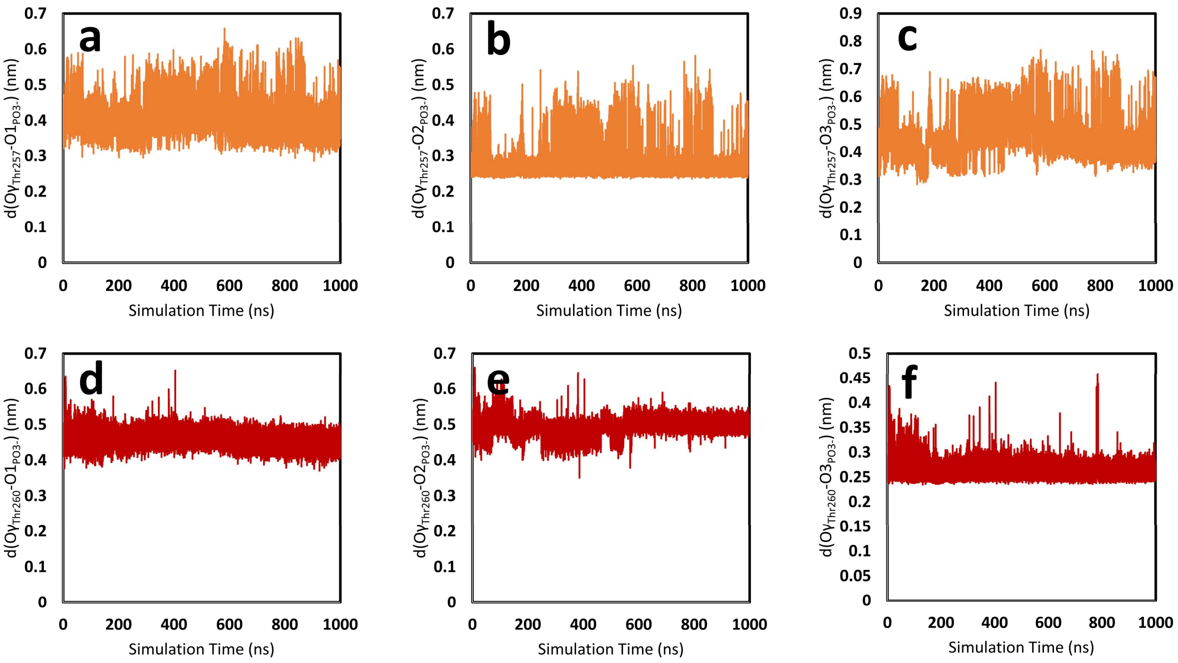

Figure S30: a,b,c. *variation of d(Oγ$_{Thr257}$-O1/2/3$_{PO3-}$) for chain A for the second 1000 ns simulation of* ***C****;* ***d,e,f.*** *variation of d(Oγ$_{Thr260}$-O1/2/3$_{PO3-}$) for chain A for the second 1000 ns simulation of* ***C****.*

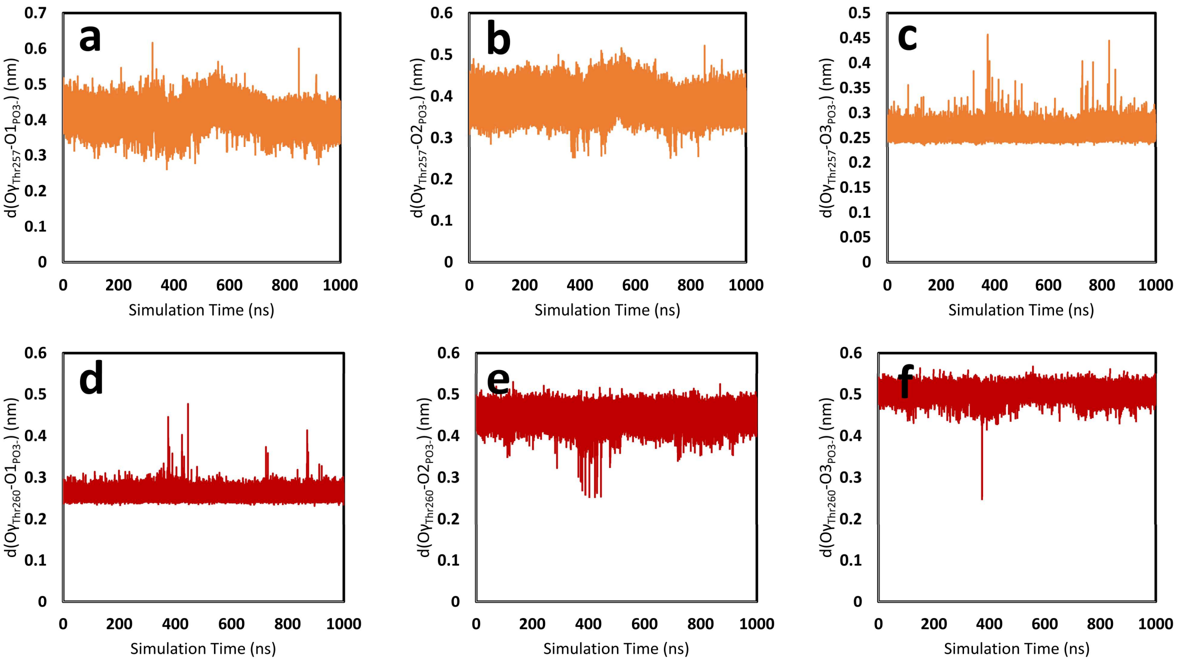

Figure S31: a,b,c. *variation of d(Oγ$_{Thr257}$-O1/2/3$_{PO3-}$) for chain B for the second 1000 ns simulation of* ***C****;* ***d,e,f.*** *variation of d(Oγ$_{Thr260}$-O1/2/3$_{PO3-}$) for chain B for the second 1000 ns simulation of* ***C****.*

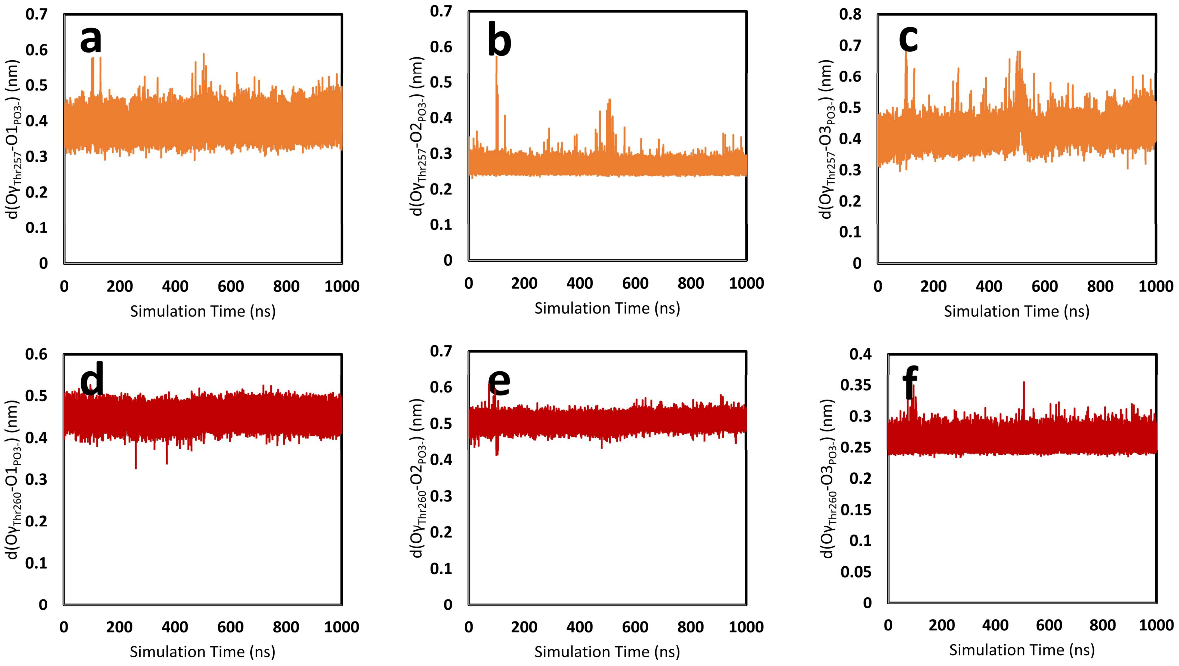

Figure S32: a,b,c. *variation of d(Oγ$_{Thr257}$-O1/2/3$_{PO3-}$) for chain A for the first 1000 ns simulation of* ***E****;* ***d,e,f.*** *variation of d(Oγ$_{Thr260}$-O1/2/3$_{PO3-}$) for chain A for the first 1000 ns simulation of* ***E****.*

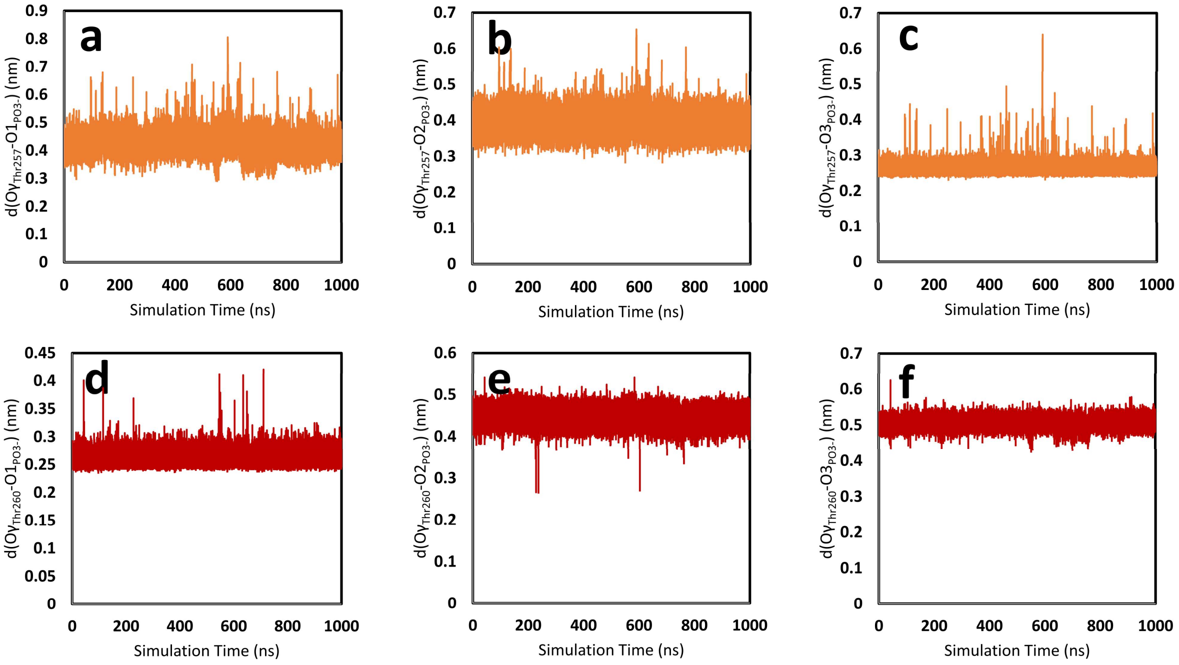

Figure S33: a,b,c. *variation of d(Oγ$_{Thr257}$-O1/2/3$_{PO3-}$) for chain B for the first 1000 ns simulation of* ***E****;* ***d,e,f.*** *variation of d(Oγ$_{Thr260}$-O1/2/3$_{PO3-}$) for chain B for the first 1000 ns simulation of* ***E****.*

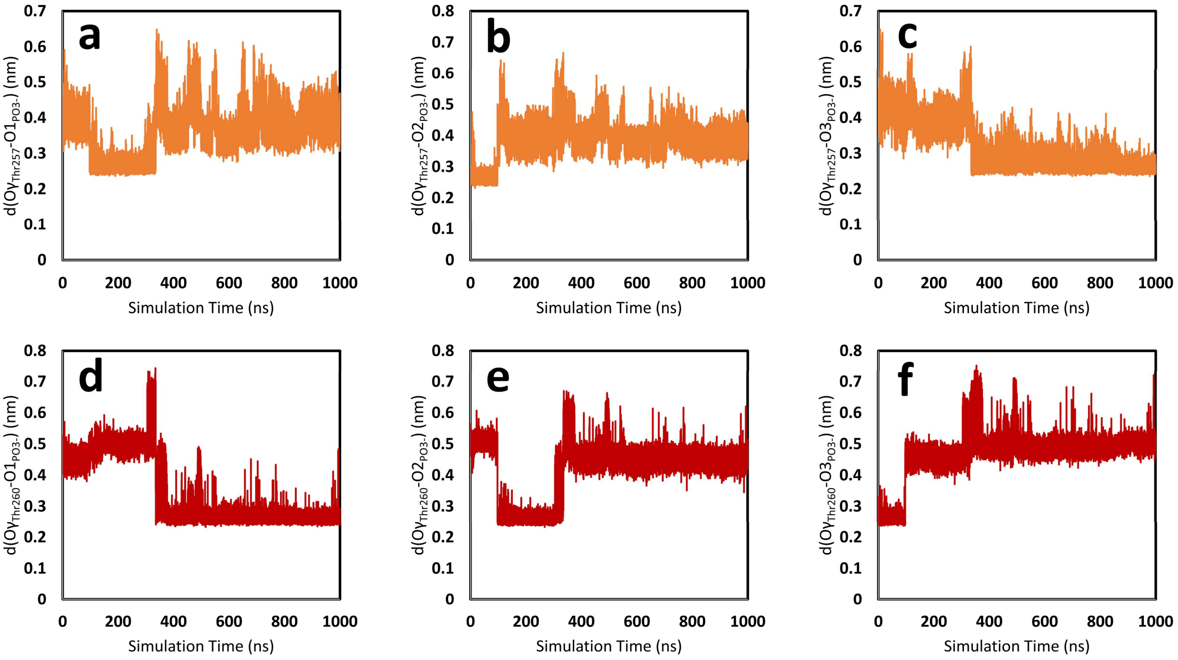

Figure S34: a,b,c. *variation of $d(O\gamma_{Thr257}\text{-}O1/2/3_{PO3-})$ for chain A for the second 1000 ns simulation of* ***E****;* ***d,e,f.*** *variation of $d(O\gamma_{Thr260}\text{-}O1/2/3_{PO3-})$ for chain A for the second 1000 ns simulation of* ***E****.*

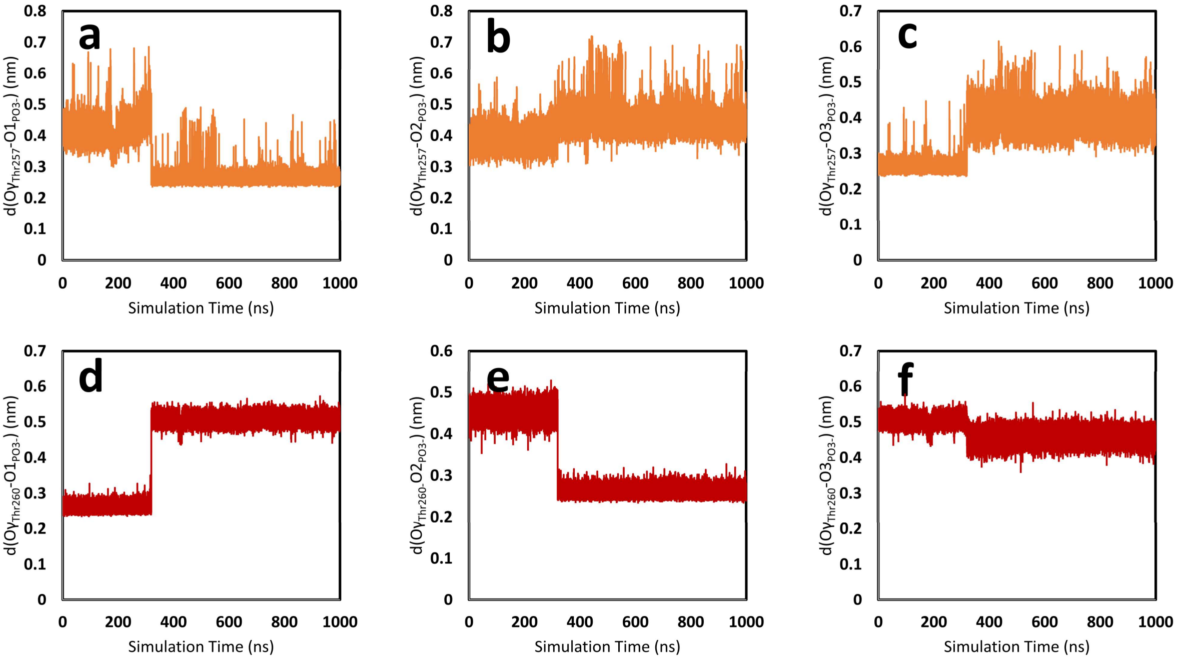

Figure S35: a,b,c. *variation of $d(O\gamma_{Thr257}\text{-}O1/2/3_{PO3-})$ for chain B for the second 1000 ns simulation of* ***E****;* ***d,e,f.*** *variation of $d(O\gamma_{Thr260}\text{-}O1/2/3_{PO3-})$ for chain B for the second 1000 ns simulation of* ***E****.*

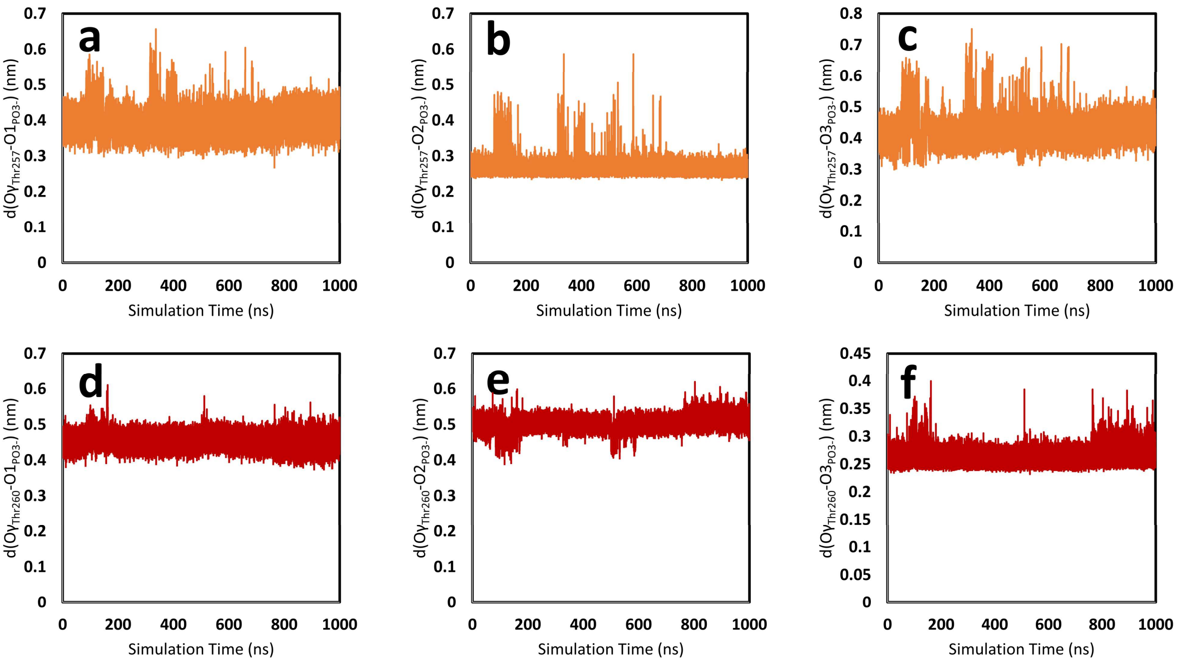

Figure S36: ***a,b,c.*** *variation of d($O\gamma_{Thr257}$-O1/2/3$_{PO3-}$) for chain A for the first 1000 ns simulation of* ***F****;* ***d,e,f.*** *variation of d($O\gamma_{Thr260}$-O1/2/3$_{PO3-}$) for chain A for the first 1000 ns simulation of* ***F****.*

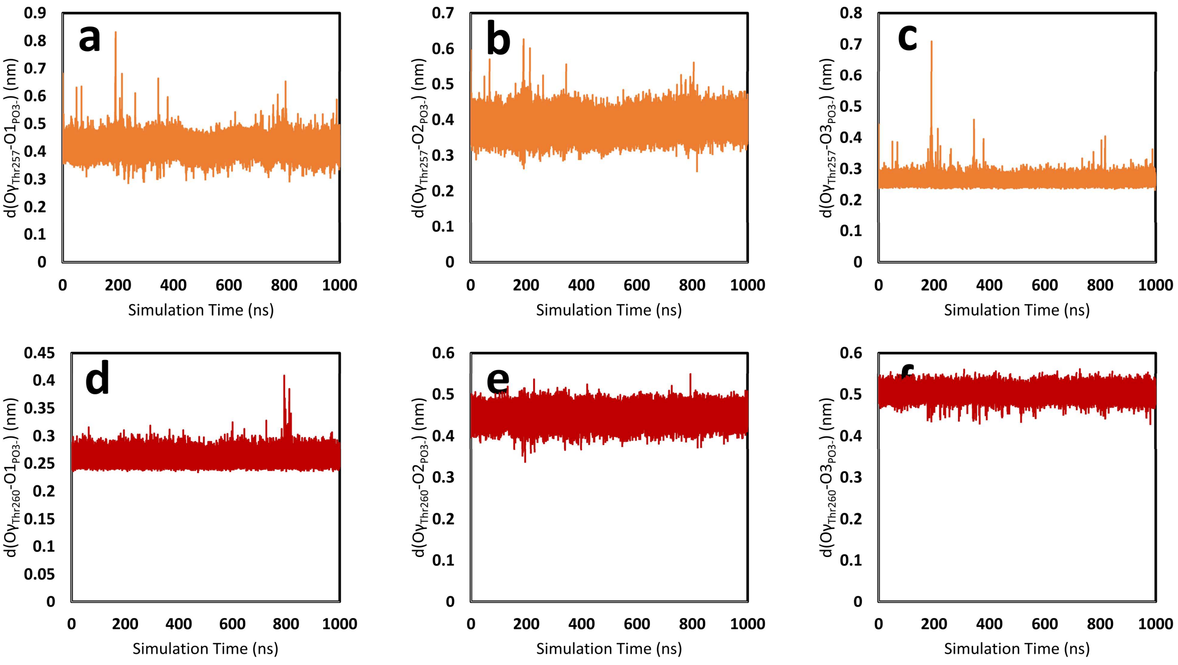

Figure S37: ***a,b,c.*** *variation of d($O\gamma_{Thr257}$-O1/2/3$_{PO3-}$) for chain B for the first 1000 ns simulation of* ***F****;* ***d,e,f.*** *variation of d($O\gamma_{Thr260}$-O1/2/3$_{PO3-}$) for chain B for the first 1000 ns simulation of* ***F****.*

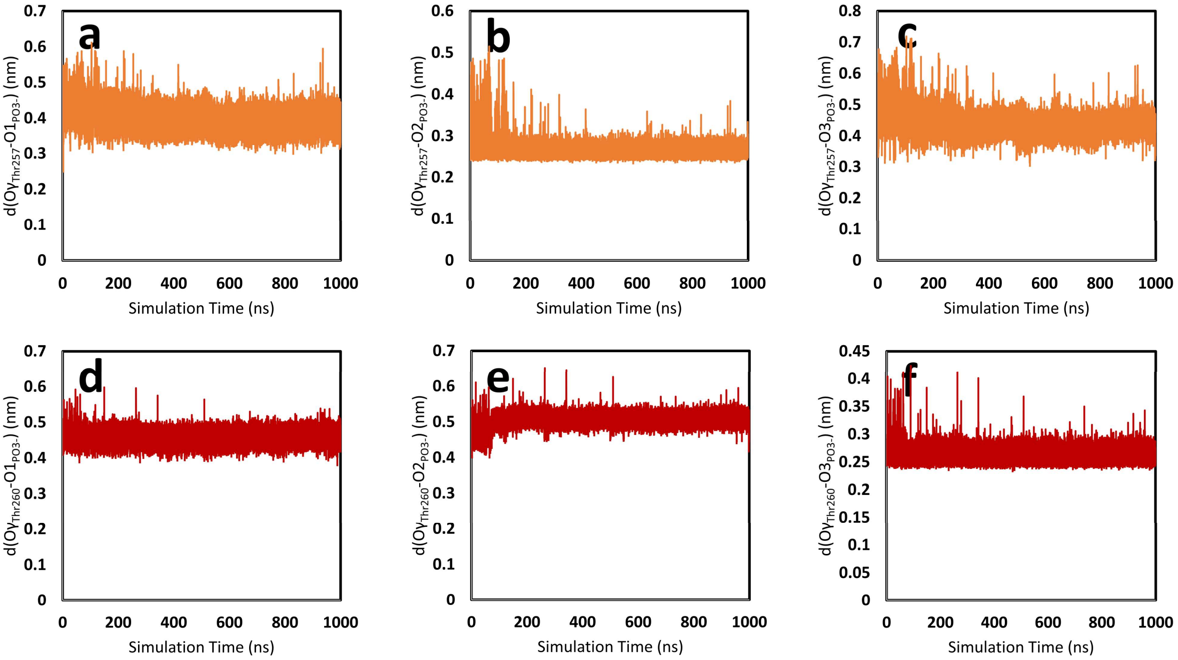

Figure S38: a,b,c. *variation of* $d(O\gamma_{Thr257}\text{-}O1/2/3_{PO3-})$ *for chain A for the second 1000 ns simulation of* ***F*****;** ***d,e,f.*** *variation of* $d(O\gamma_{Thr260}\text{-}O1/2/3_{PO3-})$ *for chain A for the second 1000 ns simulation of* ***F****.*

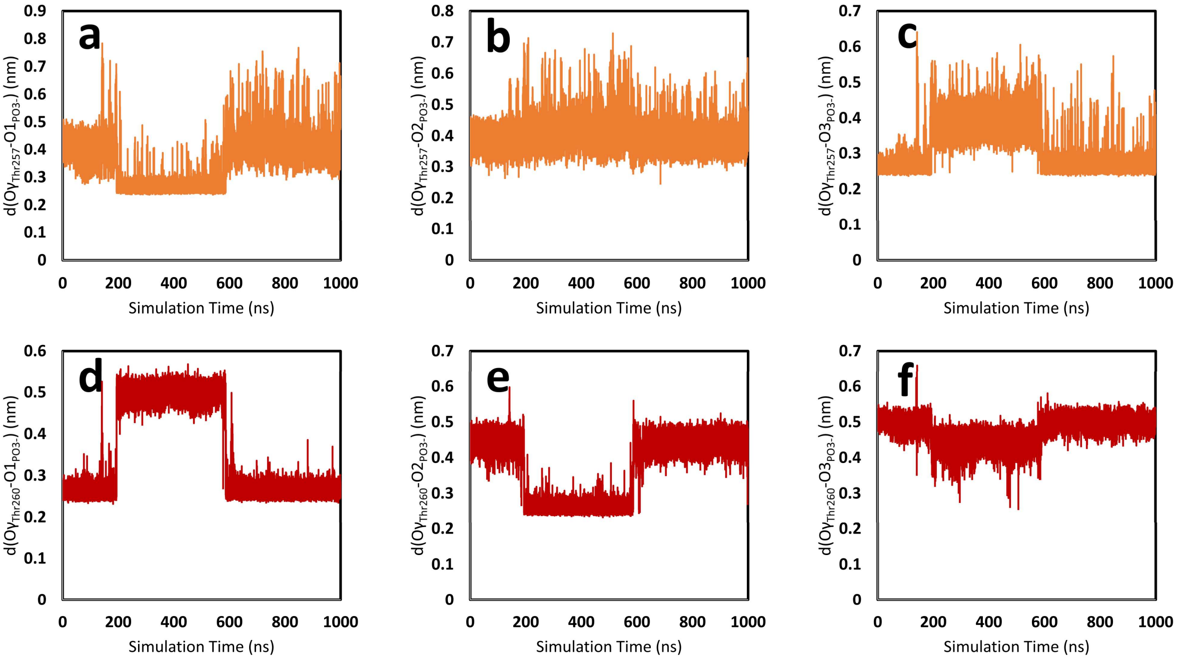

Figure S39: a,b,c. *variation of* $d(O\gamma_{Thr257}\text{-}O1/2/3_{PO3-})$ *for chain B for the second 1000 ns simulation of* ***F*****;** ***d,e,f.*** *variation of* $d(O\gamma_{Thr260}\text{-}O1/2/3_{PO3-})$ *for chain B for the second 1000 ns simulation of* ***F****.*

Table S2: *Relative Gibbs free energy changes calculated with several DFT functionals as well as the DLPNO-CCSD(T1) calculations. The left-hand side of the table shows the Gibbs free energy relative to the basal state,* ***A****, depending on whether CO or NO is the inhibitory gas. The right-hand side of the tables shows the Gibbs free energy changes associated with the steps of the inhibitory pathways.*

Functional/Method	A + CO	A + NO	D (CO)	D (NO)	B	E	C	F	$\Delta E_{A,D}$	$\Delta E_{A,B}$	$\Delta E_{D,E}$	$\Delta E_{D,F}$	$\Delta E_{B,C}$
BP86	0.0	0.0	26.2	26.2	-18.2	-9.9	-11.6	-11.8	26.2	-18.2	-36.1	-38.0	6.6
B3PW91	0.0	0.0	-1.0	-1.0	-8.3	-9.0	-5.6	-5.0	-1.0	-8.3	-8.0	-4.1	2.7
B3LYP	0.0	0.0	0.4	0.4	-8.2	-7.5	-7.6	-5.1	0.4	-8.2	-8.0	-5.5	0.6
B3LYP*	0.0	0.0	5.0	5.0	-10.7	-8.6	-8.2	-7.2	5.0	-10.7	-13.6	-12.2	2.5
BLYP	0.0	0.0	22.3	22.3	-18.2	-8.4	-15.6	-11.8	22.3	-18.2	-30.7	-34.1	2.6
OLYP	0.0	0.0	7.9	7.9	-19.2	-10.2	-19.8	-12.4	7.9	-19.2	-18.2	-20.4	-0.6
PBE	0.0	0.0	25.6	25.6	-20.7	-10.6	-14.0	-12.9	25.6	-20.7	-36.2	-38.5	6.7
TPSS	0.0	0.0	25.0	25.0	-17.2	-10.7	-10.3	-11.7	25.0	-17.2	-35.7	-36.7	6.9
PBE0	0.0	0.0	-5.2	-5.2	-8.3	-8.6	0.0	-4.3	-5.2	-8.3	-3.5	0.9	8.3
TPSSh	0.0	0.0	11.1	11.1	-12.1	-10.2	-5.6	-8.4	11.1	-12.1	-21.2	-19.5	6.6
DLPNO-CCSD(T1)	**0.0**	**0.0**	**11.2**	**11.2**	**-5.2**	**-3.9**	**-0.4**	**-1.3**	**11.2**	**-5.2**	**-15.2**	**-12.5**	**4.9**

In addition to the B3LYP and DLPNO-CCSD(T_1) calculations, a series of single-point energy calculations on a selection DFT functionals were performed on the electronic ground state of each species using the ORCA quantum chemistry package,[2] as shown in ***Table S2***. Among the DFT calculations were 4 GGA methods (BP86,[3,4] BLYP,[5] OLYP,[6] & PBE[4]), 1 meta-GGA method (TPSS[7]), 3 hybrid-GGA functionals (B3PW91,[8] B3LYP*,[9] & PBE0[10,11]), and 1 hybrid meta-GGA functional (TPSSh[7,12]). As with the DLPNO-CCSD(T_1) calculations, scalar relativistic effects were considered through ZORA[13–15], the ZORA-recontracted versions of the def2 basis sets were used (using the TZVPP/TZVP/SVP basis set combination – see ***Table S1***).[16] As auxiliary basis sets, the normal def2 family of basis sets and the segmented all-electron relativistically contracted (SARC) were used.[16,17] Grimme's D3 dispersion correction with the Becke-Johnson damping function was applied in all cases.[18,19] For pure DFT calculations, the density fitting approximation was used to solve Coulomb integrals.[20–22] For hybrid functionals, the density-fitting approximation was supplemented with the chain-of-sphere integration method to account for the Hartree-Fock exchange integrals.[23–25] The free energy correction for each species was comprised of two terms. The first is the statistical mechanics Gibbs free energy correction for each of the species at standard state (1M) taken from a frequency analysis of a hybrid B3LYP-D3 calculation performed using the TZVPP/TZVP/SVP basis set combination, where translational contributions were removed for the histidine and cysteine analogues. The second is the Gibbs free energy of solvation for each of the species, which was calculated by the difference in electronic energy for the respective functional between a vacuum and implicitly solvated model using a CPCM implicit solvent model with a protein-representative dielectric constant of $\varepsilon = 4$. Note that for the DLPNO-CCSD(T1) values reported, the Gibbs free energy of solvation was calculated using vacuum and solvated hybrid B3LYP-D3 electronic energies, as described in the manuscript.

Table S3: *Summary of raw data from ground spin state calculations on the various heme derivatives. In order, the columns are the species, the relevant spin state, the basis set combination that was used in the calculation (in this case, they are all the same), the Kohn-Sham Energy (in Hartrees), the correlation energy (in Hartrees), the sum of the previous two columns to obtain the total energy (in kcal/mol), the spin state gaps relative to the singlet or doublet depending on the species, and the obtained ground spin state based on these calculations.*

Species	Spin State	Basis Set Combination	KS Energy (Ha)	Correlation Energy (Ha)	Total Energy (kcal/mol)	Spin State Gaps (kcal/mol)	Ground Spin State
A	**Singlet**	TZVP/SVP	-2882.627653	-5.225123209	-1812127.617	0	**Singlet**
	Triplet	TZVP/SVP	-2882.651862	-5.194160413	-1812123.379	4.237814347	
	Quintet	TZVP/SVP	-2882.704649	-5.134225873	-1812118.894	8.72320129	
B	**Doublet**	TZVP/SVP	-2787.024548	-4.851742519	-1751902.373	0	**Doublet**
	Quartet	TZVP/SVP	-2787.093065	-4.748703562	-1751880.71	21.66251233	
	Sextet	TZVP/SVP	-2787.149858	-4.693802816	-1751881.897	20.47532124	
C	**Doublet**	TZVP/SVP	-2387.279376	-4.670145513	-1500948.325	0	**Doublet**
	Quartet	TZVP/SVP	-2387.441334	-4.472889186	-1500926.175	22.14982757	
	Sextet	TZVP/SVP	-2387.495396	-4.430348816	-1500933.405	14.92007064	
D	**Singlet**	TZVP/SVP	-2482.946414	-4.967205478	-1561165.796	0	**Quintet**
	Triplet	TZVP/SVP	-2483.010862	-4.913718909	-1561172.674	-6.878271598	
	Quintet	TZVP/SVP	-2483.090117	-4.853470955	-1561184.602	-18.80561276	
E	**Singlet**	TZVP/SVP	-2595.659596	-5.368790991	-1632145.313	0	**Singlet**
	Triplet	TZVP/SVP	-2595.575765	-5.37214684	-1632094.815	50.49830911	
	Quintet	TZVP/SVP	-2595.722029	-5.251897248	-1632111.138	34.17459941	
F	**Doublet**	TZVP/SVP	-2612.116309	-5.460741905	-1642529.6	0	**Doublet**
	Quartet	TZVP/SVP	-2612.224009	-5.315059365	-1642505.766	23.8340426	
	Sextet	TZVP/SVP	-2612.33515	-5.223460859	-1642518.028	11.571415	

Table S4: *Summary of the RMSF based on the position of the α-carbons of the main residues in the signalling pathway found in human CBS. In order, the columns are the species, which simulation run it was, the chain (A or B), and the RMSF values for the relevant residues along with the mean and standard deviation for the residue for each of the species.* ***A**, **C**, **E**, or **F**.*

Species	**Run**	**Chain**	**RMSF (nm)**					
			Cys52	*His65*	*Asn149*	*Thr257*	*Thr260*	*Arg266*
A	*1*	A	0.046	0.190	0.095	0.075	0.063	0.074
		B	0.043	0.158	0.116	0.089	0.063	0.065
	2	A	0.033	0.115	0.087	0.105	0.068	0.061
		B	0.037	0.105	0.128	0.082	0.069	0.068
		Mean ± SD	**0.04 ± 0.006**	**0.142 ± 0.039**	**0.107 ± 0.019**	**0.088 ± 0.013**	**0.066 ± 0.003**	**0.067 ± 0.005**
C	*1*	A	0.388	1.057	0.145	0.107	0.102	0.119
		B	0.484	1.117	0.153	0.111	0.104	0.111
	2	A	0.410	1.156	0.151	0.105	0.086	0.132
		B	0.225	0.859	0.122	0.094	0.075	0.090
		Mean ± SD	**0.377 ± 0.109**	**1.047 ± 0.132**	**0.142 ± 0.014**	**0.104 ± 0.007**	**0.092 ± 0.014**	**0.113 ± 0.017**
E	*1*	A	0.310	0.250	0.073	0.078	0.064	0.073
		B	0.243	0.149	0.072	0.081	0.071	0.075
	2	A	0.219	0.229	0.074	0.078	0.069	0.092
		B	0.177	0.162	0.074	0.084	0.068	0.087
		Mean ± SD	**0.237 ± 0.055**	**0.198 ± 0.049**	**0.073 ± 0.001**	**0.08 ± 0.003**	**0.068 ± 0.003**	**0.082 ± 0.009**
F	*1*	A	0.437	0.165	0.141	0.126	0.108	0.098
		B	0.430	0.319	0.120	0.083	0.072	0.096
	2	A	0.414	0.161	0.089	0.076	0.062	0.089
		B	0.244	0.160	0.089	0.086	0.078	0.075
		Mean ± SD	**0.381 ± 0.092**	**0.201 ± 0.079**	**0.11 ± 0.026**	**0.093 ± 0.023**	**0.08 ± 0.02**	**0.09 ± 0.01**

Table S5: *Hydrogen bond percentage for the Asn149–O⁻(PLP) hydrogen bond. The percentage is calculated on the basis of the following hydrogen bond assignment criteria:* $\angle(N\delta_{Asn149}\text{-}H\delta_{Asn149}\text{-}O12_{PLP}) > 100$ *degrees, and* $d(N\delta_{Asn149}\text{-}O12_{PLP}) < 0.35$ *nm.*[26] *Plots of the data used to calculate these percentages are shown in* ***Figures S8 – S23****. In order, the columns are the species, which simulation run it was, the chain (A or B), and hydrogen bond percentage.*

Species	Run	Chain	Hydrogen Bond %
A	*1*	A	87
		B	92
	2	A	73
		B	81
C	*1*	A	83
		B	38
	2	A	75
		B	25
E	*1*	A	89
		B	86
	2	A	83
		B	86
F	*1*	A	71
		B	13
	2	A	88
		B	79

Additional Data

Gaussian16 DFT Optimisation Convergence Criteria

Table S6: *The optimisation convergence criteria used for all Gaussian16 optimisations. These criteria are the default for optimisations in Gaussian16.*

	Threshold	
Maximum Force	0.000450	a.u.
RMS Force	0.000300	a.u.
Maximum Displacement	0.001800	a.u.
RMS Displacement	0.001200	a.u.

ORCA5 DLPNO Parameters

Table S7: *The DLPNO parameters available in ORCA5. Shown in bold (keyword: NormalPNO) are the DLPNO parameters used for all DLPNO-CCSD(T_1) calculations.*

Setting	$T_{CutPairs}$	T_{CutDO}	T_{CutPNO}	T_{CutMKN}	MP2 Pair Treatment
LoosePNO	10^{-3}	2×10^{-2}	1.00×10^{-6}	10^{-3}	Semicanonical
NormalPNO	$\mathbf{10^{-4}}$	$\mathbf{1 \times 10^{-2}}$	$\mathbf{3.33 \times 10^{-7}}$	$\mathbf{10^{-3}}$	**Semicanonical**
TightPNO	10^{-5}	5×10^{-3}	1.00×10^{-7}	10^{-3}	Full iterative

hCBS Crystal Structures Data

Table S8: *Summary of important parameters relating to the available crystal structures for hCBS. In order, the columns are the Protein Data Bank ID, the resolution (in Angstroms), the R-Value Free, any comments relating to the choice of crystal structure in this work, and the relevant reference. Shown in bold are the details of the crystal structure used in this work.*

pdb-id	*Resolution (Å)*	*R-Value Free*	*Comments*	*Ref.*
1JBQ	2.60	0.296	Wild-type, reduced model (only heme and catalytic domain), missing residues in catalytic domain	27
1M54	2.90	0.365	Mutated, reduced model (only heme and catalytic domain), missing residues in catalytic domain	28
4COO	**2.00**	**0.201**	**Wild-type, all four domains, only some missing residue atoms in catalytic domain**	**29**
4L0D	2.97	0.284	Mutated, all four domains, only some missing residue atoms in catalytic domain	30
4L3V	3.63	0.232	Wild-type, all four domains, no missing atoms or residues in catalytic domain	30
4L27	3.39	0.244	Mutated, all four domains, no missing atoms or residues in catalytic domain	30
4L28	2.63	0.281	Mutated, all four domains, missing residues in catalytic domain	30
5MMS	2.80	0.221	Mutated, reduced model, missing residues in catalytic domain	31

References

1 F. Neese and E. F. Valeev, *J. Chem. Theory Comput.*, 2011, **7**, 33–43.

2 F. Neese, F. Wennmohs, U. Becker and C. Riplinger, *The Journal of Chemical Physics*, 2020, **152**, 224108.

3 A. D. Becke, *Phys. Rev. A*, 1988, **38**, 3098–3100.

4 J. P. Perdew, K. Burke and M. Ernzerhof, *Phys. Rev. Lett.*, 1996, **77**, 3865–3868.

5 C. Lee, W. Yang and R. G. Parr, *Phys Rev B Condens Matter*, 1988, **37**, 785–789.

6 N. C. HANDY and A. J. COHEN, *Molecular Physics*, 2001, **99**, 403–412.

7 J. Tao, J. P. Perdew, V. N. Staroverov and G. E. Scuseria, *Phys. Rev. Lett.*, 2003, **91**, 146401.

8 A. D. Becke, *The Journal of Chemical Physics*, 1993, **98**, 5648–5652.

9 M. Reiher, O. Salomon and B. Artur Hess, *Theoretical Chemistry Accounts: Theory, Computation, and Modeling (Theoretica Chimica Acta)*, 2001, **107**, 48–55.

10 J. P. Perdew, M. Ernzerhof and K. Burke, *The Journal of Chemical Physics*, 1996, **105**, 9982–9985.

11 C. Adamo and V. Barone, *The Journal of Chemical Physics*, 1999, **110**, 6158–6170.

12 V. N. Staroverov, G. E. Scuseria, J. Tao and J. P. Perdew, *The Journal of Chemical Physics*, 2003, **119**, 12129–12137.

13 E. van Lenthe, J. G. Snijders and E. J. Baerends, *The Journal of Chemical Physics*, 1996, **105**, 6505–6516.

14 E. van Lenthe, E. J. Baerends and J. G. Snijders, *The Journal of Chemical Physics*, 1993, **99**, 4597–4610.

15 E. van Lenthe, E. J. Baerends and J. G. Snijders, *The Journal of Chemical Physics*, 1994, **101**, 9783–9792.

16 D. A. Pantazis, X.-Y. Chen, C. R. Landis and F. Neese, *J. Chem. Theory Comput.*, 2008, **4**, 908–919.

17 F. Weigend and R. Ahlrichs, *Phys. Chem. Chem. Phys.*, 2005, **7**, 3297–3305.

18 S. Grimme, J. Antony, S. Ehrlich and H. Krieg, *The Journal of Chemical Physics*, 2010, **132**, 154104.

19 S. Grimme, S. Ehrlich and L. Goerigk, *Journal of Computational Chemistry*, 2011, **32**, 1456–1465.

20 J. L. Whitten, *The Journal of Chemical Physics*, 1973, **58**, 4496–4501.

21 O. Vahtras, J. Almlöf and M. W. Feyereisen, *Chemical Physics Letters*, 1993, **213**, 514–518.

22 B. I. Dunlap, J. W. D. Connolly and J. R. Sabin, *The Journal of Chemical Physics*, 1979, **71**, 3396–3402.

23 F. Neese, F. Wennmohs, A. Hansen and U. Becker, *Chemical Physics*, 2009, **356**, 98–109.

24 R. Izsák and F. Neese, *The Journal of Chemical Physics*, 2011, **135**, 144105.

25 B. Helmich-Paris, B. de Souza, F. Neese and R. Izsák, *The Journal of Chemical Physics*, 2021, **155**, 104109.

26 E. N. Baker and R. E. Hubbard, *Progress in Biophysics and Molecular Biology*, 1984, **44**, 97–179.

27 M. Meier, M. Janosik, V. Kery, J. P. Kraus and P. Burkhard, *The EMBO Journal*, 2001, **20**, 3910–3916.

28 S. Taoka, B. W. Lepore, Ö. Kabil, S. Ojha, D. Ringe and R. Banerjee, *Biochemistry*, 2002, **41**, 10454–10461.

29 T. J. McCorvie, J. Kopec, S.-J. Hyung, F. Fitzpatrick, X. Feng, D. Termine, C. Strain-Damerell, M. Vollmar, J. Fleming, J. M. Janz, C. Bulawa and W. W. Yue, *Journal of Biological Chemistry*, 2014, **289**, 36018–36030.

30 J. Ereño-Orbea, T. Majtan, I. Oyenarte, J. P. Kraus and L. A. Martínez-Cruz, *Proceedings of the National Academy of Sciences*, 2013, **110**, E3790–E3799.

31 J. B. Vicente, H. G. Colaço, F. Malagrinò, P. E. Santo, A. Gutierres, T. M. Bandeiras, P. Leandro, J. A. Brito and A. Giuffrè, *Oxidative Medicine and Cellular Longevity*, 2017, **2017**, e8940321.